Elsevier Editorial System(tm) for Catalysis Today

Manuscript Draft

Manuscript Number:

Title: Recent Progress of Photocatalytic Membrane Reactors in Water Treatment and in Synthesis of Organic Compounds. A review.

Article Type: SI: Photocatalysis

Keywords: Photocatalytic membrane reactor;
Photodegradation of pollutants;
Photosynthesis of organic compounds;
Pressurized membrane photoreactors;
Submerged membrane photoreactors;
Photocatalytic membrane contactors.

Corresponding Author: Prof. Raffaele Molinari,

Corresponding Author's Institution:

First Author: Raffaele Molinari

Order of Authors: Raffaele Molinari; Cristina Lavorato; Pietro Argurio

Abstract: Hybrid processes combining membrane separation and heterogeneous photocatalysis represent an exciting technology because each technique complements the advantages and overcomes the challenges of the other. This combination gives plants set-up named Photocatalytic Membrane Reactors (PMRs). PMRs can be designed in two configurations: reactors in which the catalyst is suspended in the reaction mixture and reactors that utilize the photocatalyst immobilized/deposited on membrane surface, giving a photocatalytic membrane. PMRs allow to perform a variety of chemical reactions (e.g. degradation or synthesis of organic compounds) and separation in one step thus minimizing environmental and economic impacts in agreement with the Green Chemistry principles. Different PMR configurations (pressurized, submerged, with photocatalytic membrane, photocatalytic reactors with membrane distillation, with membrane dialysis, with a pervaporation membrane) have been applied in water treatment for degradation of different organic pollutants (such as dyes, pharmaceuticals and other pollutants) and in the synthesis of organic compounds (such as phenol, vanillin and phenylethanol). The main experimental results of the different applications will be described and critically examined in this review.

Recent Progress of Photocatalytic Membrane Reactors in Water Treatment and in Synthesis of Organic Compounds. A review.

Raffaele Molinari*, Cristina Lavorato, Pietro Argurio

Department of Environmental and Chemical Engineering, University of Calabria

Via P. Bucci, Cubo 45/A, I-87036 Arcavacata di Rende (CS), Italy,

Ph. +39 0984 496699, email: raffaele.molinari@unical.it

Highlights

- PMRs represent a green system for water treatment as well as for organic synthesis
- In PMRs the photocatalyst can be both in suspension and entrapped in/on a support.
- PMRs have been successfully tested in the removal of dyes and drugs from water
- Submerged PMRs with oxygen bubbling limit membrane fouling
- A PMR allows to improve the overall productivity in organic synthesis

*Graphical Abstract (for review)

Recent Progress of Photocatalytic Membrane Reactors in Water Treatment and in Synthesis of Organic Compounds. A review.

Raffaele Molinari*, Cristina Lavorato, Pietro Argurio

Department of Environmental and Chemical Engineering, University of Calabria

Via P. Bucci, Cubo 45/A, I-87036 Arcavacata di Rende (CS), Italy,

Ph. +39 0984 496699, email: raffaele.molinari@unical.it

Graphical abstract

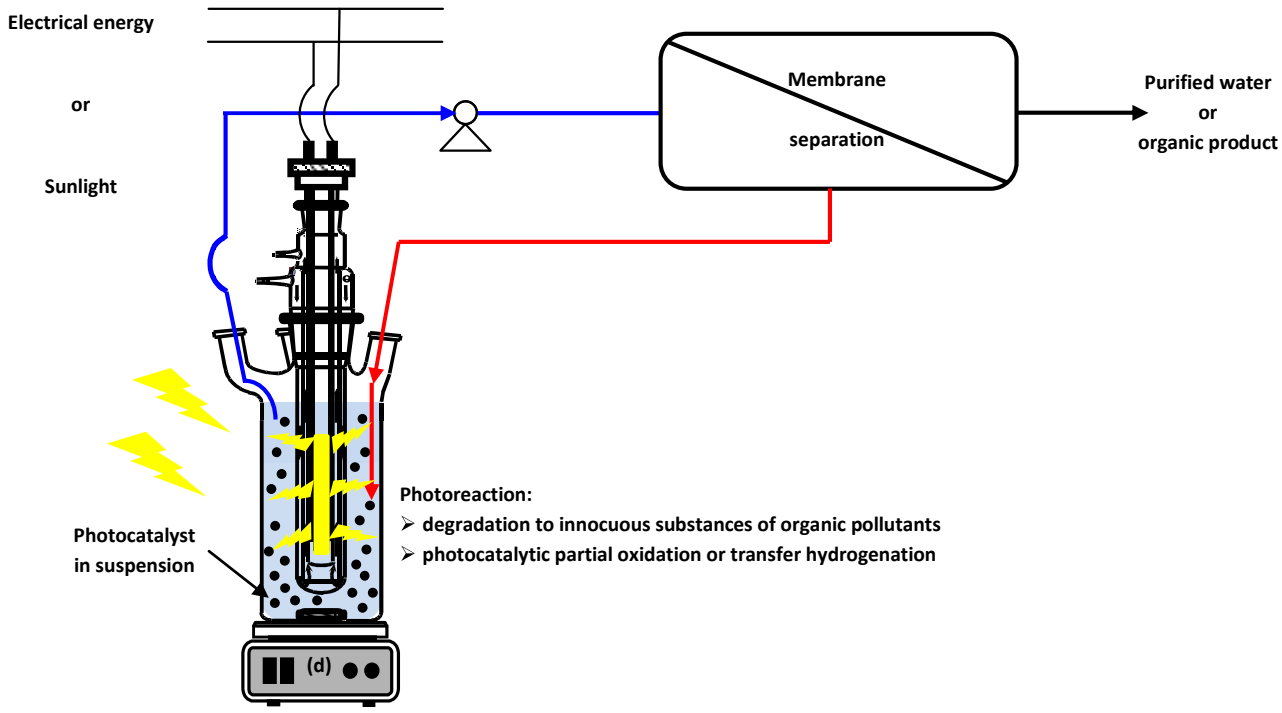

Recent Progress of Photocatalytic Membrane Reactors in Water Treatment and in Synthesis of Organic Compounds. A review.

Raffaele Molinari*, Cristina Lavorato, Pietro Argurio

Department of Environmental and Chemical Engineering, University of Calabria

Via P. Bucci, Cubo 45/A, I-87036 Arcavacata di Rende (CS), Italy,

Ph. +39 0984 496699, email: raffaele.molinari@unical.it

Submitted to Catalysis Today, March 2016

* corresponding author

Abstract

Hybrid processes combining membrane separation and heterogeneous photocatalysis represent an exciting technology because each technique complements the advantages and overcomes the challenges of the other. This combination gives plants set-up named Photocatalytic Membrane Reactors (PMRs). PMRs can be designed in two configurations: reactors in which the catalyst is suspended in the reaction mixture and reactors that utilize the photocatalyst immobilized/deposited on membrane surface, giving a photocatalytic membrane. PMRs allow to perform a variety of chemical reactions (e.g. degradation or synthesis of organic compounds) and separation in one step thus minimizing environmental and economic impacts in agreement with the Green Chemistry principles.

Different PMR configurations (pressurized, submerged, with photocatalytic membrane, photocatalytic reactors with membrane distillation, with membrane dialysis, with a pervaporation membrane) have been applied in water treatment for degradation of different organic pollutants (such as dyes, pharmaceuticals and other pollutants) and in the synthesis of organic compounds (such as phenol, vanillin and phenylethanol). The main experimental results of the different applications will be described and critically examined in this review.

Keywords: Photocatalytic membrane reactor; Photodegradation of pollutants; Photosynthesis of organic compounds; Pressurized membrane photoreactors; Submerged membrane photoreactors; Photocatalytic membrane contactors.

1. Introduction

Heterogeneous photocatalysis is an advanced oxidation process (AOP) based on the use of light and a semiconductor (the photocatalyst) to generate the oxidizing/reducing species. It has been extensively studied since about four decades, when Fujishima and Honda [1] discovered the photocatalytic splitting of water on TiO_2 electrodes.

It has been object of a large amount of studies related to environment recovery by the total degradation to innocuous substances of organic and inorganic pollutants [2, 3], the removal of toxic metals, and for synthesis [4]. It is a discipline that includes a large variety of reactions [5]: partial or total oxidations, metal deposition, water detoxification, gaseous pollutant removal, bactericidal action [6-8], and, recently, dehydrogenation and hydrogenation (e.g. hydrogen transfer) [5].

The main difference of photocatalysis compared to conventional catalysis is the photonic activation mode of the catalyst, which replace the thermal activation [6]. The electronic structure of a semiconductor is characterized by a conduction band (CB) and a valence band (VB) separated by a band gap of energy (Eg). When semiconductors are excited by photons with energy ($h\nu$) equal to or higher than their band gap energy level (Eg), valence electrons (e^-) are promoted from VB to CB, thus leaving a positive hole (h+) in the VB.

For a generic semiconductor (SC), this step can be expressed as:

$$SC + h\nu \rightarrow SC\ (e^- + h^+) \quad (1)$$

In the absence of suitable electron and/or hole scavengers, the photo-generated electrons and holes can recombine in bulk or on surface of the semiconductor within a very short time, releasing energy in the form of heat or photons. Electrons and holes that migrate to the surface of the semiconductor without recombination can, respectively, reduce and oxidize the adsorbed substrate.

The overall photocatalytic process can be summarized in four steps: i) absorption of light followed by the separation of the electron–hole couple; ii) adsorption of the reagents; iii) redox (reduction and oxidation) reaction; iv) desorption of the products.

Thanks to favorable energetic of its band structure, relatively high quantum yield, stability under irradiation and low cost and availability, TiO_2 represents the archetypical photocatalyst, virtual synonym for photocatalysis. Nevertheless, this material does not present photo-response under visible light illumination because of its wide band gap, taking advantage of only less than about 5% of the solar energy. Thus its potential as a green technology cannot be entirely fulfilled. In the last years a great number of new photocatalysts have been synthesized and tested as possible alternatives to TiO_2 [9, 10] particularly in view of solar application.

Because of the highly unselective reactions involved in the photocatalytic processes, these ones have been widely studied in remediation processes, in which organic and inorganic pollutants in liquid and gas phases are totally degraded to innocuous substances. However, in last decade some studies have been carried out on the application of photocatalysis for synthesis such as selective reduction and oxidation. These studies demonstrated that high selectivity could be obtained in photo-oxidation and photo-reduction processes in comparison to conventional methods by appropriately selecting or modifying some photocatalytic parameters, as the semiconductor

surface or the excitation wavelength. In this framework, the photocatalytic oxidation of organic compounds has been largely studied because the most common semiconductors have VB edges more positive than oxidation potentials of most organic functional groups [11]. Instead, photocatalytic reductions are less frequently found, because the reducing power of a CB electron is significantly lower than the oxidizing power of a VB hole [2, 12].

Important characteristics of photocatalysis, making it in agreement with the Green Chemistry principles, consist in the mild operating conditions (ambient temperature and pressure, very few auxiliary additives and short reaction times) and in the possibility to abate refractory, very toxic and non biodegradable molecules [13, 14]. Besides, photocatalysis: i) avoids the use of environmentally and unhealthy dangerous heavy metal catalysts by using safer photocatalysts (mainly TiO_2); ii) avoids the use of strong oxidants/reducing agents; iii) permits the real destruction of the contaminants with the formation of innocuous by-products; iv) can be applied to a wide range of substrates in aqueous, solid and gaseous phase; v) is applicable to solutions at low concentrations; v) offers a good alternative to the energy-intensive conventional treatment methods; vi) permits to use renewable solar energy; vii) can be combined with other physical and chemical technologies (e.g. membrane separations).

Despite the above mentioned advantages, use of photocatalytic processes in the industry is still limited for three different reasons [15]: i) recombination of photo-generated electron/hole pairs which dissipate their energy as heat; ii) fast backward reaction; iii) difficulty to employ visible light, limiting the effectiveness of utilization of solar energy. The latter involves significant energy consumption for artificially irradiating the system, having an important impact on the economic competitiveness of the process. The main approaches studied to solve these problems, enhancing the photocatalytic activity and promote the visible light response, consist in: i) addition of electron donors or electron scavengers, able to react irreversibly with the photo-generated VB holes or CB electrons, respectively; ii) doping of the semiconductor with a noble metal (e.g. Pt, Au, Pd, Rh, Ni, Cu, Ag) so that photo-promoted electrons can be transferred from CB of the semiconductor to metal particles deposited on its surface, thus avoiding electron-hole recombination; iii) dye sensitization.

An important aspect to be considered in view of large scale applications is the recovery of the catalyst from the reaction environment. Photocatalytic Membrane Reactors (PMRs) represent a very promising approach to obtain this requirement.

A PMR can be defined as a device existing in various configurations which combine a photocatalyst and a membrane to produce chemical transformations. PMRs are an useful "green" technology which improve the potentialities of classical photoreactors (PRs) and those of membrane processes (separation at molecular level) giving a synergy for both technologies thus minimizing environmental and economical impacts [4, 16]. The membrane permits continuous operation in systems in which the recovery of the photocatalyst (immobilized or in suspension), the reaction and the separation of the products simultaneously occur. Higher energy efficiency, modularity and easy scale up are some other potential advantages of PMRs.

PMRs can be built in two configurations: (i) PMRs that employ powdered TiO_2 suspended in the reaction mixture and (ii) PMRs that utilize TiO_2 immobilized on a substrate material (e.g. glass, quartz, mesoporous materials, stainless steel or polymers) acting as a membrane.

Based on the greater available active surface area compared to immobilized system, the configurations with suspended catalyst have been largely used in literature, founding them more efficient than that using immobilized catalysts [17-20].

In a PMR the membrane can assume many roles. The appropriate choice of the membrane (material and type) and membrane module configuration is mainly determined by the type of photocatalytic reaction. First of all, it is important to choose a membrane with complete catalyst rejection thus maintaining it in the reaction environment. Besides, when the process is used for the degradation of organic pollutants, the membrane must be able to reject the substrates and their intermediate products, which otherwise pass in the permeate. Thus the residence time of the molecules to be degraded in the photocatalytic step is increased, guarantying the complete degradation of recalcitrant substances. When the photocatalytic process is used as a synthetic pathway, the main objective of the membrane can be the selective separation of the product, e.g. minimizing its successive oxidation which leads to undesirable by-products.

In the present paper the application of different PMR configurations (pressurized, submerged, with catalytic membrane, photocatalytic membrane contactor) in water treatment for degradation of organic pollutants (e.g. dyes, pharmaceutical compounds and other pollutants) and in the synthesis of organic compounds (e.g. phenol, vanillin and phenylethanol) will be critically examined and discussed.

2. Photodegradation of organic pollutants in water

Our modern life-style has led to the presence of various synthetic compounds in aqueous effluents, resulting in environment pollution. As a consequence environmental laws and regulations have also become more stringent in order to protect both human health and the environment and they will become more and more restrictive in the next years. Various directives suggest using the green chemistry concepts and clean technologies inside the manufacturing processes to protect the environment. Conventional chemical (e.g. adsorption, chemical oxidation) and biological treatments to clean-up water often fail to remove the majority of organic pollutants because of their high resistance (recalcitrant compounds), resulting in high concentrations discharged in treated effluents. Thus, there is a need for the development of new technologies that can remove these emerging hazardous compounds in water and wastewater.

In this context photocatalytic processes represent a promising alternative green process [21-23] since, as consequence of the highly unselective reactions involved in the photocatalytic processes, a wide range of organic pollutants can be totally degraded (i.e. mineralized) in very small and harmless species (Equation (2)), minimizing the use of chemicals and avoiding sludge production and its disposal.

$$\text{Organic molecules} \xrightarrow{OH^{\bullet}} \text{Oxidation products} \xrightarrow{OH^{\bullet}} \text{C to } CO_2\text{, H to } H_2O\text{, N to nitrate, S to sulphate, P to phosphate} \quad (2)$$

Photocatalytic processes have been reported in literature for the mineralization of different compounds as dyes [24-26], pesticides and herbicides [27, 28], pharmaceutical compounds [29-32], hormones [33], various toxic organic molecules [34-36].

In the following section PMRs applications in the removal of organic pollutants from water will be presented and critically discussed.

2.1 PMRs in the photodegradation of Azo Dyes in aqueous media

Dyes are organic compounds used in textile, food and drug industries, and their abatement represents one of the main problems in the treatment processes because generally they are very stable toxic compounds [37-39]. Some authors stated the wastewater produced by the textile industry as the most polluting among the industrial sectors [40-42]. It has been estimated that during the dyeing process the losses of colorants to the environment can reach 10–50% of the initial one. Azo-dyes represent the most common dyes actually employed in textile industries and a relevant problem is related to the presence of these chemicals in the environment because some

azo dyes can show toxic effects, especially carcinogenic and mutagenic events [43]. In order to meet the limitation imposed by the current legislation, the aqueous effluents coming from industrial plants that use dyes in their processes are usually treated by physical-chemical, oxidative or, most commonly, active sludge biochemical processes [44]. Homogeneous oxidation treatments are generally effective towards the destruction of the chromophore structures and the water discoloration, but a complete mineralization of the dye is often not achieved.

In Table 1 various experimental works regarding the application of PMRs in the photodegradation of dyes contained in aqueous systems are summarized. Some of them are based on the use of slurry type photoreactors, in which the photocatalyst is suspended in the reaction environment, other on the use of the photocatalyst immobilized in/on the membrane thus forming a catalytic membrane.

198 Table 1: Experimental works on the application of PMRs in the photodegradation of dyes contained in aqueous media.

Photocatalyst(*)	(**)	Membrane	Irradiation	Pollutant (***)	Main Results	Drawbacks	Ref
TiO_2-P25	Susp	PES NF	UV	CR PB	99%/45% dye removal (CR/PB) 30 L m^{-2} h^{-1} permeate fluxes TMP = 3.5-7 bar	Low PB rejection Membrane fouling causing a 60% flux decline during continuous run	[45]
ZnO nanoparticles	Susp	NF or UF	UV	Industrial wastewater from printing presses	100% color removal, 100% turbidity reduction, 100% suspended solid rejection with NF membrane ca 13 L m^{-2} h^{-1} permeate fluxes TMP = 6 bar	Membrane fouling causing a 65% flux decline Permeation of photocatalyst and dye molecules with UF membrane	[46]
TiO_2-P25	Susp	HFM-UF	UV	MB	95% degradation, 64% mineralization 98% and 74% dye and TOC removal	Progressive performance degradation due to TiO_2 agglomeration	[47]
TiO_2 (AV-01)	Susp	HFM-MF	UV	AR1	100% color removal, ca. 76% COD removal, ca. 60% TOC removal 40 L m^{-2} h^{-1} critical flux, TMP = -0.105 bar 0.5 h^{-1} back-flushing frequency for 5 min at -40 l m^{-2} h^{-1} to control fouling	Dead end filtration mode Rapid flux decline due to TiO2 particles deposition on the membrane	[48]
TiO_2	Imm	Ceramic UF	UV	DB168	72% degradation, 82% dye removal 82 L m^{-2} h^{-1} permeate flux TMP = 0.5 bar	Not complete dye degradation	[49]
N doped TiO_2 GO doped TiO_2	Imm	Ceramic UF	UV Visible	MB MO	N-TiO_2 membrane under UV 57% and 29% MB and MO rejection 38.18 and 34.31 L m^{-2} h^{-1} permeate flux TMP = 4.6 and 3.7 bar	Two or more permeate recycle needed to obtain satisfactory rejections. Dead end filtration mode. Synthetic effluent.	[50]

N doped TiO_2	Imm	Ceramic UF	UV	4BS	99% dye removal 25 L m^{-2} h^{-1} permeate flux TMP = 4 bar	Rapid formation of cake layer due to the dead end filtration mode. Poor photo activity under vis light.	[51]
TiO_2-P25 Lab made TiO_2 GO doped TiO_2	Imm	UF cellulose	UV Visible	MO	GO doped TiO_2 65% degr., 31% miner. (UV) 19% degr., 9% miner. (Visible) 90 and 81 L m^{-2} h^{-1} permeate flux under UV and visible light	Dead end filtration mode NaCl leads to a slight decrease in dye degradation Lower photocatalytic efficiency compared to suspended photocatalyst	[52]
Alginate-TiO_2 fibers	Imm	γ-alumina UF tube	UV	MO	40% dye removal during continuous flow experiments 5.8-7.9 L m^{-2} h^{-1} permeate flux TMP = 14 bar	Gradual degradation of alginate-TiO_2 fibers. High dye concentration in the permeate	[53]
Ag/TiO_2 nanofiber	Imm	Glass filter	Solar light	MB	80% degr., 80% miner. (30 min); complete miner. (80 min) ca. 7 L m^{-2} h^{-1} permeate flux TMP = 0.5 bar	Bench scale level Dead end filtration mode Results obtained with synthetic effluent	[54]
TiO_2-P25	Susp	DCMD		AR18 AY36 DG99	No fouling: TiO_2 don't affect permeate flux (14.2 L m^{-2} h^{-1}) 100% rejection of the Dye	Lower permeate flux and higher energetic consumption of MD with respect to NF and UF	[55, 56]

(*) GO: Graphene Oxide. (**) susp: suspended; imm: immobilized. (***) CR : Congo Red; PB: Patent Blue; AR1: Acid Red 1; MB: Methylene Blue; DB168: Direct black 168; 4BS: Direct Fast Scarlet 4BS; MO: Methyl orange; AR18: Acid Red 18; AY36: Acid Yellow 36; DG99: Direct Green 99.

2.1.1. Suspended photocatalyst into slurry type photoreactor

Molinari et al. [45] studied the photo-degradation process of Congo Red (CR) and Patent Blue (PB) in a suspended PMR using TiO_2-P25 as the photocatalyst and NTR 7410 NF membrane to maintain the photocatalyst in the reaction environment. The results, obtained during continuous tests with CR, reported in Fig. 1, show that use of the nanofiltration (NF) membrane was beneficial because it acted as a barrier for both the catalyst and the substrate. Indeed the obtained permeate contained a very low concentration of CR (ca. 0.1%) with respect to 500 mg/L of the feed. Thus it was demonstrated that it is possible to successfully treat highly concentrated solutions of dyes by means of a continuous process, which is an important feature of a PMR. Permeate flux throughout the run decreased from the initial value of 74.2 L m^{-2} h^{-1} to the value of 29.8 L m^{-2} h^{-1}, because of membrane fouling, that is the principal drawback of the proposed PMR.

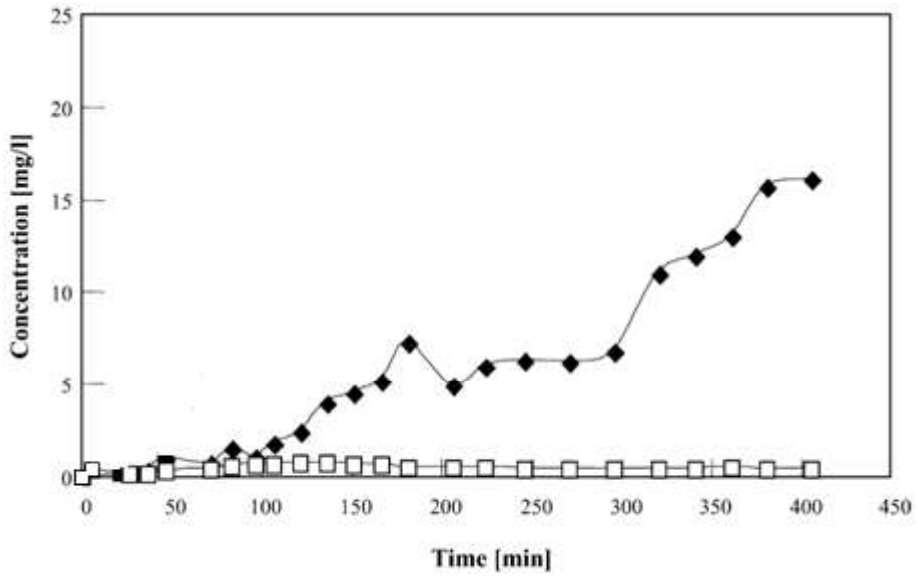

Fig. 1. Congo Red concentration of in the retentate and in the permeate versus time: (♦) retentate; (□) permeate. (V = 500 mL; T = 303 K; C_0 = 0 mg L^{-1}; $C(O_2)$ = 22 ppm; TiO_2 amount = 1 g L^{-1}; C_{feed} = 500 mg L^{-1}; initial permeate flux: $J_{p,in}$ = 74.2 L m^{-2} h^{-1}; final permeate flux: $J_{p,fin}$ = 29.8 L m^{-2} h^{-1}; lamp: 125W medium pressure Hg immersed lamp; initial pH 6.42, P = 3.5 bar), elaborated from Molinari et al. [45].

The lower performance obtained in the case of PB degradation (the permeate contained ca. 11% of PB amount with respect to the feed) clearly evidenced that the used NF membrane was not the best choice for this substrate. Then the right choice of the membrane is a key step to increase PMR performance.

A different photocatalyst, ZnO nanoparticles self-synthesized via precipitation method, was tested by Hairom et al. [46] in a suspended PMR for industrial dye wastewater treatment. Both NF and ultrafiltration (UF) membranes (Polypiperazine amide NF membrane Trisep TS40 and Polyamide UF membrane Trisep GMSP, from GE Osmonics, USA) were tested and their performances in obtaining cleaner water production and ZnO nanoparticles retaining were compared. The results evidenced that an industrial wastewater from printing presses was successfully treated in the proposed system. Operating pH played a significant role in controlling the photocatalytic efficiency and fouling behavior in the PMR system. pH 11 and 0.1 g L^{-1} of ZnO loading were the optimum operational condition. A severe fouling was observed at pH 2, 7 and 8 because of the weak electrostatic repulsion between the membrane surface, ZnO particles and the dye in the wastewater being all the pHs near to their isoelectric point. The NF membrane gave the best performance in terms of color removal (100%), chemical oxygen demand (92%), turbidity reduction (100%) and total suspended solid rejection (100%). A 65% normalized flux reduction was obtained, because of photocatalyst accumulation on membrane surface. Worse performance was obtained by using the UF membrane owing to the permeation of nanosized ZnO and dye molecules across the membrane pores.

Both Molinari et al. [45] and Hairom et al. [46] observed a 60-65% flux decline in their experiments. Then the PMR with photocatalyst in suspension could be interesting by an application point of view for the decontamination of highly concentrated effluents produced in the dyes-related industries once the problems related to membrane fouling, mainly caused by the photocatalyst deposition on the membrane, will be opportunely minimized.

The use of a hollow fiber membrane (HFM) and membrane back-flushing represents a useful approach to overcome this problem. In 1999 Sopajaree et al. [47] tested the possibility to integrate a slurry-based heterogeneous photoreactor with a pressurized HFM-UF unit, for the degradation of Methylene Blue (MB) by using TiO_2 Degussa P25. Complete photocatalyst separation from treated effluent was observed, evidencing that the used HFM-UF unit permitted to maintain the photocatalyst into the reacting environment. The progressive flux decrease observed during the operation, due to photocatalyst deposition on the membrane, was controlled by membrane back-flushing.

A satisfactory dye removal was obtained (98%), but a 26% of total organic carbon (TOC) passed in the permeate, since some photodegradation intermediate crossed the membrane. Besides, a systematic decrease of photocatalytic performance was observed during subsequent cycles of

operation (86% and 42% MB and TOC removal, respectively, after the 10^{th} cycle of operation). Dynamic light scattering measurements demonstrated the caking of suspended TiO_2 during the UF process and the subsequent re-dispersion stage promoted agglomeration of the TiO_2 particles, resulting in progressive diminution of the photocatalytic activity.

The performance of HFM systems can be enhanced by operating in de-pressurized mode, i.e. the permeate is sucked inside HFM and the catalyst deposition is reduced with air bubbling and membrane back-flushing. On the basis of this Kertèsz et al. [48] tested a PMR, obtained by integrating a photoreactor with a submerged HFM module, in the photocatalytic degradation of Acid Red 1 (AR1) in an aqueous dispersion of TiO_2. Wastewater containing AR1 was successfully decolorized, validating the feasibility of the proposed system in treating industrial wastewaters containing dyes. Complete photocatalyst recovery was obtained. The rapid flux decline, caused also by the dead-end filtration mode, was controlled by air bubbling, thus achieving a dual purpose: oxygen saturation, which promotes photodegradation reactions, and TiO_2 particles removal from the surface of the fibers [57-59]. A sustainable permeate flux of 40 L m^{-2} h^{-1} was found for the investigated system. Below this value reversible membrane fouling was detected, which was easily removed by membrane back-flushing with the permeate, while above this value irreversible fouling was observed. Fouling of the submerged membrane can be controlled (not avoided) by optimizing the operating parameters and, in particular, membrane back-flushing parameters, i.e. frequency, duration and intensity. Membrane back-flushing also allows maintaining the required catalyst concentration in the reaction mixture.

When a PMR with suspended photocatalyst is employed, the overall plant set-up can be divided in two zones: i) the photocatalytic reactor zone (i.e. the photoreactor) where the photocatalyst is irradiated and the photocatalytic reaction takes place; ii) the membrane separation zone (i.e. the membrane separation unit) where the confining of the photocatalyst and of the un-reacted substrate in the reactor happens. On the basis of this, the distribution of the PMR's volumes between these two zones is another important design parameter that needs to be optimized [45, 48].

Summarizing, the use of PMR systems with suspended photocatalyst could be interesting by an application point of view, for the decontamination of industrial dye wastewater because the membrane permits: i) the separation and reuse of the photocatalyst; ii) the control of the residence time of the pollutant and its photodegradation intermediate in the photoreactor, thus obtaining dye mineralization and high quality permeate; iii) the operation in continuous mode

[60]. Besides, considering the accessible active surface, systems with suspended catalyst are potentially more efficient than immobilized systems, as reported in literature [17-20].

Despite these achievements, the slurry-type membrane systems possess some drawbacks, such us:

i) fouling, which main consequences are permeate flux decline and stacking and accumulation of the photocatalyst nanoparticles on the membrane surface, also resulting in decreasing the performance of the photocatalytic degradation;
ii) requirement of additional time and expensive treatment (usually filtration) if the separation and recovery of the photocatalyst particles from the retentate is required;
iii) light scattering by both catalytic particles and dissolved organic compounds present in the slurry.

However, the use of submerged membrane modules, coupled with air bubbling and membrane back-flushing, seems to be a valuable choice to limit very well membrane fouling effects.

2.1.2. Immobilized photocatalyst in/on the membrane (Photocatalytic membrane)

Photocatalyst immobilization, by obtaining a photocatalytic membrane (PM), swapping from the conventional slurry-type systems, could improve the performance of purification technology based on coupling photocatalysis and membrane filtration in view of real applications. In such a system, the membrane has the simultaneous task of supporting the photocatalyst as well as acting as a selective barrier for the species to be degraded.

However, some drawbacks of PMs are: i) moderate loss of photoactivity also related to the low photocatalyst availability to irradiation; ii) necessity to irradiate the surface of the membrane, resulting in technical difficulties and in possible membrane photodegradation; iii) restricted processing capacities owing to mass transfer limitations and iv) unsatisfactory system lifetime owing to the possible catalyst deactivation and wash out. Then it is fundamental to manufacture systems with opportune porosity and effective dispersion of the catalyst particles.

About 30 years ago, Anderson and co-workers [61, 62] published pioneering feasibility studies of concurrent membrane separation and photocatalytic oxidation using supported TiO_2-based membranes.

More recently, Molinari et al. [45] considered the possibility to entrap the photocatalyst in a polymeric membrane, finding a lower efficiency with respect to the suspended configuration, because the presence of the polymer around the particles of catalyst reduces the effective surface

area. Another disadvantage of the system with photocatalyst entrapped in polymeric membranes is the risk of a possible membrane oxidation by •OH radicals attack.

Inorganic membranes are preferable over the conventional polymeric materials, owing to their excellent thermal, chemical, and mechanical stability. Zhang et al. [49] successfully prepared TiO_2/Al_2O_3 composite membranes with photocatalytic capability by the sol–gel technique. The obtained PMs permitted to obtain 82% removal efficiency of Direct Black 168 after 300 min of continuous operation under UV irradiation. The TiO_2/Al_2O_3 composite PMs permitted photocatalytic reaction and separation simultaneously, obtaining a high permeate flux (82 L m^{-2} h^{-1}) by using a low pressure (0.5 bar), thanks to the high porosity and pore size of the membrane, but the permeate quality was not excellent.

The necessity to develop visible-light-active photocatalytic systems represents another fundamental key point in view of large scale application of PMR systems, permitting the use of a greener light source (the sun). Athanasekou et al. [50] prepared highly active photocatalytic ceramic UF membranes testing they in a photocatalytic device operating in continuous dead-end flow conditions under near-UV/vis and visible light irradiation. Methylene blue (MB) and methyl orange (MO) were the tested azo-dyes. Nitrogen doped TiO_2 (N-TiO_2), grafene oxide doped TiO_2 (GO-TiO_2) and organic shell layered TiO_2 were deposited on the external and internal surface of UF mono-channel monoliths by dip-coating. Better results were achieved with the N-TiO_2 membrane (57% and 29% degradation against MB and MO, respectively) under UV irradiation. These results, unsatisfactory by an environmental point of view, evidenced that the used UF membrane is not adequate for dye rejection, despite the photocatalyst deposition.

The GO-TiO_2 membrane appeared the best one in terms of energetic cost of the process, since for MB it provided 63% of the rejection of N-TiO_2 membrane while consuming only 28% of the respective energy. So a higher dye rejection can be achieved with a lower power energy consumption by recycling the permeate of the GO-TiO_2 membrane two or more times. However more recycling of the permeate to obtain rejection similar to that one obtained by NF/photocatalytic systems can be a drawback.

Wang et al. [51] prepared and tested a more efficient N-TiO_2 ceramic composite PM. It was synthesized with the dip coating method, as reported by Athanasekou et al. [50], but the coating process was repeated 7 times, so that composite membranes with an average pore size of about 2 nm, which is adequate for dye capture, were synthesized. SEM and XRD analyses showed that N doping, inhibiting the growth of TiO_2 crystal grains, permitted to obtain smaller TiO_2 nanocrystals

with a huge surface and an interfacial area, which improved the catalytic activity. During the filtration experiments, carried out in dead end mode under UV light, a good permeation flux (25 L m^{-2} h^{-1}, over 96% of pure water flux), very high dye rejection (close to 99%) and good membrane stability after several time reuse were obtained. Although those results, rapid formation of cake layer, also due to the dead end filtration mode and concentration polarization, which also caused dye rejection decline, were observed. Besides, the N-TiO_2 composite membranes showed poor photoactivity under visible light.

Since real industrial effluents (e.g. from textile or printing industry) usually contain salts and dissolved organic matter together dyes, the effects of these substances on photocatalytic membrane performances have also to be considered. Potential effects of salts and dissolved organic matter presence on system performance can be: i) decrease of photocatalytic performance; ii) increase of membrane fouling.

From this consideration, Pastrana-Martinez et al. [52] studied the effect of dissolved NaCl on photocatalytic membrane performance. Three photocatalysts, i.e. commercial TiO_2 P25, lab-made TiO_2 and GO-TiO_2, were immobilized on a flat sheet cellulose membrane. Obtained PMs, named M-P25, MTiO_2 and M-GOT, were tested in the degradation and mineralization of MO under both near UV-Vis and visible light irradiation working in dead end continuous mode. Distilled water (DW), simulated brackish water (SBW, 0.5 g L^{-1} NaCl) and seawater (SW, 35 g L^{-1} NaCl) were considered as aqueous matrixes. The results, summarized in Table 2 in the case of DW, show that the M-GOT system was the best one. M-P25 and M-TiO_2 membranes were practically inactive under Visible light, while the addition of GO, decreasing the band gap, results in a moderate visible light activity. The presence of NaCl (0.5 g L^{-1}) lead to a slight decrease in MO degradation, regardless of the membranes employed, since Cl^- ions acted as holes and hydroxyl radical scavengers. However, M-GOT system remained the better one, with 52 and 13% MO degradation for near UV-Vis and Visible light irradiation, respectively.

Table 2: Photocatalytic degradation of MO in distilled water (DW) in continuous mode under near UV-Vis and visible light irradiation (data from [52]).

	MO degradation (%)		
Light irradiation	M-P25	M-TiO_2	M-GOT
Near UV-Vis	51	39	65
Visible	5	4	19

Despite these encouraging results, the authors underline that slurry-type photoreactors posses higher catalytic efficiency in comparison with the tested photocatalytic membranes, as reported also in other works [63, 64].

An interesting and promising approach, in view of enhancing the photocatalytic activity of PM, is based on the implementation and use of fiber based membranes.

Those systems, thanks to their enhanced porosity and effective dispersion and stabilization of the catalyst nanoparticles, could represent a radical solution to the previous reported intrinsic problems of photocatalytic membranes. On this concept, Papageorgiu et al. [53] proposed and tested Ca alginate polymer fibers to effectively disperse and stabilize TiO_2 P25 in their matrix. Properties like the high transparency of the alginate matrixes and the possibility to induce extended porosity make the Ca alginate polymer fibers good candidate to be used in photocatalytic applications.

The Ca alginate/TiO_2 fibers were prepared by the dry/wet spinning process in a spinning set-up. Batch tests were performed to evaluate their photocatalytic performance using 100 cm of the fibers cut in 10 cm pieces placed in a glass tube containing a MO solution. The results showed that Ca alginate/TiO_2 fibers possess higher efficiency for the removal of MO from polluted water than bulk TiO_2 powder, because of their high surface area and their good MO adsorption capacity combined with the excellent dispersion and stability of the TiO_2 nanoparticles into the biopolymer matrix. A gradual degradation of the Ca alginate/TiO_2 polymer fibers, caused by the attack of the generated OH• radicals on the polymeric material, was observed.

Continuous flow experiments were carried out by coupling the composite Ca alginate/TiO_2 porous fibers with a photocatalytic UF membrane obtained by deposition of TiO_2 nanoparticles, grown with the Chemical Vapor Deposition (CVD) method, on both the surfaces of a γ-alumina UF support. In Fig. 2 the hybrid photocatalytic/UF experimental set-up is reported. It consists of three concentric tubes placed in the vertical direction. The inner tube is the photocatalytic UF membrane. The intermediate and external tubes are made of Plexiglas, and define an outer flow channel (the annular space between the tubes) where polluted water is fed in the lumen of the transparent Ca alginate/TiO_2 polymer fibers.

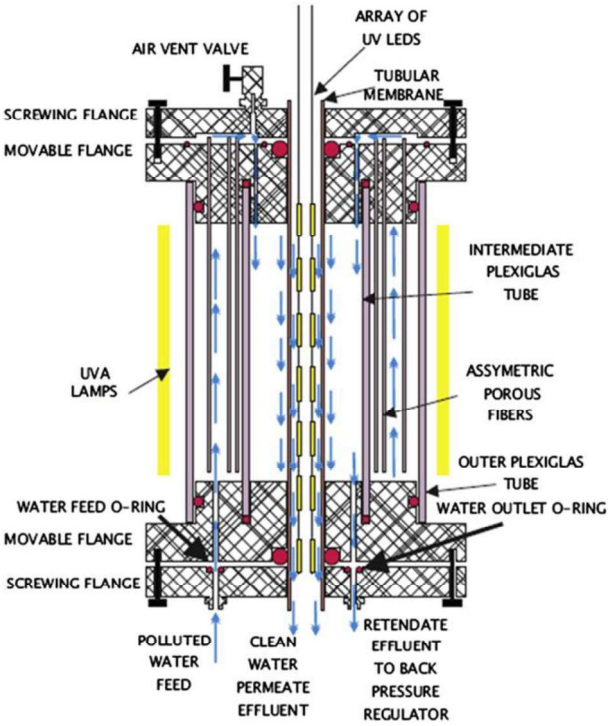

Fig. 2. Schematization of the photocatalytic membrane system used in the hybrid photocatalytic/ultrafiltration tests [53].

Obtained results showed that the presence of TiO_2/Ca alginate fibers (not permeable) as pretreatment stage of the photocatalytic UF membrane led to an enhancement of the MO removal efficiency with respect to the use of the PM alone. Thanks to the presence of the membrane, the degraded biopolymer was retained into the retentate. Besides, the addition of these fibers in the process increased the permeate flux across the membrane, resulting in an increased recovery rate at steady state. Despite the above mentioned advantages, dye removal was low (40%).

Degradation of the TiO_2/Ca alginate fibers and poor dye removal are some aspect to be solved in view of industrial application, since they affect both permeate quality and photocatalytic system lifetime. Despite these important limitations, the development of TiO_2 nanofiber eliminated the problem of particles agglomeration which is a bottle neck in photocatalysis with TiO_2 powder because it is detrimental to the preservation of particle size, surface area and its reusable life-span.

To increase the photocatalytic performances of TiO_2 nanofiber and the photocatalytic response under visible light, metal doping of TiO_2 photocatalyst can be considered. This photocatalyst modification also enhances the photo-efficiency owing to the efficient electron-hole separation

[65-67]. Liu et al. [54] tested a Ag/TiO_2 nanofiber photocatalytic membrane in photocatalytic disinfection and degradation applications. During the first step of preparation, Ag nanoparticles with size around 50 nm were successfully deposited on the surface of electrospun TiO_2 nanofibers. A vacuum filtration of Ag/TiO_2 nanofiber suspension on a glass filter and a hot press process permitted to obtain the photocatalytic membrane. The results evidenced that the proposed method permitted to obtain a photocatalytic membrane in which both membrane fouling and loss of catalyst efficiency were avoided. The latter was obtained since Ag nanoparticles were homogeneously dispersed on TiO_2 nanofibers, while maintaining sufficient active sites, as shown by the BET specific surface area of Ag/TiO_2 nanofibers which increased from 85.6 m^2/g (pure TiO_2 nanofibers) to 102.3 m^2/g.

The photocatalytic property of the Ag/TiO_2 nanofiber membrane was investigated in the degradation of the dye MB under solar irradiation. The results, summarized in Table 3, show that the Ag/TiO_2 nanofiber membrane posses significantly enhanced photocatalytic activity under solar irradiation with respect to pure TiO_2 nanofiber membrane and commercial P25 deposited membrane. 30 min solar irradiation could remove nearly 80% of MB, and complete mineralization was achieved after 80 min. This result evidence that the decreased photocatalytic activity due to mass transfer limitation classically linked to photocatalyst immobilization was avoided by using nanofiber membranes, because of the high specific surface area.

Table 3: MB degradation rate constant under solar irradiation by using different TiO_2 based photocatalytic membrane (data from [54]).

	MB degradation rate constant (min^{-1})
P25 membrane	0.0076
TiO_2 nanofiber membrane	0.0137
Ag/TiO_2 nanofiber membrane	0.0211

The Ag/TiO_2 nanofiber membrane showed an excellent reusability, since no photocatalytic degradation activity was observed after five successive photodegradation tests. Meanwhile, the excellent intrinsic antibacterial capability of Ag/TiO_2 nanofiber membrane could be beneficial for the membrane biofouling control, which is an important feature in view of real applications.

2.1.3. Coupling of photocatalysis and membrane distillation

The previous reported effects of membrane fouling, representing intrinsic limits of the conventional slurry-type systems, can be avoided by coupling photocatalysis and membrane distillation (MD). MD is a separation process based on the principle of vapor–liquid equilibrium in which: i) the non-volatile components (e.g. ions, macromolecules, etc.) are retained on the feed side; ii) the volatile components pass through a porous hydrophobic membrane and then they condense in a cold distillate (usually distilled water).

Mozia et al. [55, 56] studied the possibility to use a PMR obtained by integrating photocatalysis and direct contact membrane distillation (DCMD) for degradation of different azo dyes (Acid Red 18 (AR18), Acid Yellow 36 (AY36) and Direct Green 99 (DG99)) contained in aqueous solution, by using TiO_2-P25 and a membrane module equipped with 9 polypropylene capillary membranes (effective area 0.014 m^2).

The results evidenced that the presence of TiO_2 in the feed solution did not affect the permeate flux (0.34 m^3 m^{-2} d^{-1}, which is the same obtained by using ultrapure water as feed) regardless of TiO_2 concentration and dye applied.

The results of degradation tests, reported in Fig. 3, show the highest effectiveness of photodecomposition was obtained in the case of AR18, while the most difficult compound to be degraded was AY36, having the lowest molecular weight.

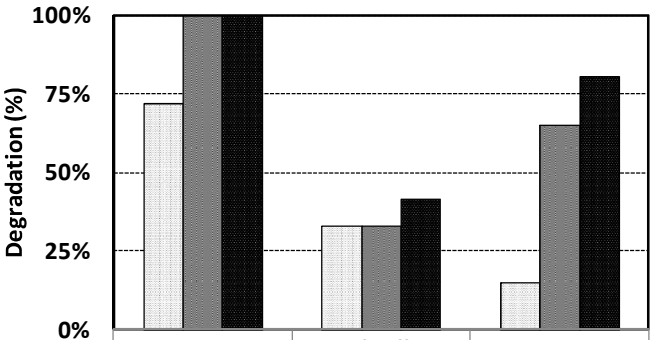

	Acid Red 18	Acid Yellow 36	Direct Green 99
0.1 g/L	71.67%	32.67%	14.73%
0.3 g/L	100.00%	32.67%	65.22%
0.5 g/L	100.00%	41.47%	80.54%

Fig. 3. Photodegradation of Acid Red 18, Acid Yellow 36 and Direct Green 99 in the PMR obtained by coupling photocatalysis and DCMD (evaluated at 5 h hours, data from [56]).

480 Complete rejection of the dye and other non-volatile compounds (organic molecules and inorganic
481 ions) was achieved. Some volatile compounds crossed the membrane, as indicated by Total
482 Organic Carbon (TOC) measurements, into the distillate. However, the amount of these substances
483 remained in the range 0.4-1.0 mg L^{-1}, meaning that the product (distillate) was practically pure
484 water. Then the hybrid process coupling the photocatalysis and DCMD can be a very promising
485 method for the removal of organic compounds, such as azo dyes from water, since the MD
486 membrane is a very effective barrier for the catalyst particles as well as the non-volatile
487 compounds present in the feed solution.
488 Similar results were obtained by Huo et al. [21] in the removal of MO from aqueous solutions by
489 using BiOBr photocatalyst under visible light irradiation. The prepared hierarchical flower-like
490 BiOBr microspheres showed high efficiency for MO photodegradation, thanks to their large
491 specific surface area, their visible-light absorbance and the lower recombination of photo-
492 generated electrons and holes. Both the organic pollutants and the catalyst were retained feed
493 side, resulting in a high quality permeate. The water flux was constant during the
494 photodegradation experiments and no membrane fouling was observed.
495 The results obtained by Mozia et al. [55, 56] and Hou et al. [21] evidenced that coupling
496 photocatalysis with MD offer the advantage of reducing the significant fouling compared with
497 pressure driven membrane processes, such as UF and NF.
498 One of the most severe obstacles for the full-scale implementation of the DCMD systems is high
499 energy demand for heating the feed solution, representing a cost item not negligible compared to
500 other process costs. When comparing the coupling of photocatalysis with MD vs. pressure driven
501 process, the pumping costs of the latter have to be compared with the energy cost of MD, also
502 considering its advantages in terms of fouling reduction. On this aspect, to the best of our
503 knowledge, there are no data in literature.
504 It should be also mentioned that MD is still a process under development. Therefore, today the
505 pressure driven membrane processes have more potential full scale applications than MD.
506
507 **2.2. PMR in the photodegradation of pharmaceuticals in aqueous media**
508 In the last years the interest for the presence of pharmaceutically active compounds (PhACs) and
509 their metabolites in waterways has increased significantly not only because of the threat posed to
510 health and safety of the aquatic life but also due to their continuous accumulation in aquatic
511 environment and development of antibiotic-resistant microbial strains [68-70]. These compounds

512 reach the aquatic environment as refusals of the hospital structures, pharmaceutical industries,
513 municipal sewage treatment plants, as well as residues of their use in agriculture and breeding
514 [71, 72]. Several investigations [73, 74] showed that PhACs and their active metabolites are not
515 completely removed during conventional wastewater treatments and they are detectable in the
516 environment with concentration levels up to the $\mu g\ L^{-1}$ [75, 76]. These amounts are lower than
517 maximum concentrations reported for typical industrial contaminants, but their toxicological
518 chronic effects, due to the continuous exposure, are unknown. On this basis, the demand for
519 developing efficient systems, alternative to the traditional purification methods, to remove PhACs
520 from water has assumed a great research interest [77]. PMRs could represent a useful solution to
521 this problem.
522 In Table 4 some PMR applications in the photodegradation of pharmaceuticals contained in
523 aqueous media are summarized.
524

525 Table 4: PMR applications in the photodegradation of pharmaceuticals contained in aqueous media.

Photocatalyst(*)	(**)	Membrane	Irradiation	Pollutant (***)	Main Results	Drawbacks	Ref
TiO_2-P25	Susp	NF membrane module	Sunlight	LIN	R% = 93.64-97.78% depending on drug concentration. By operating in continuous, very low concentration of both substrate and intermediates in the permeate	TOC accumulation in the reacting volume due to incomplete drug mineralization.	[78]
TiO_2-P25	Susp	NF	UV	FUR RAN	R% = 10–60% and 5–30% for FUR and RAN, respectively, in the dark.	No drugs rejection during photocatalytic tests: inadequacy of the membrane Tests carried our only in recirculation regime	[29]
TiO_2-P25	Susp	NF or UF	UV	GEM TAM	Pressurized system: 100% GEM removal; 60% drug miner.; permeate flux 38.6 L h^{-1} m^{-2} (6 bar) Depressurized system: 100% catalyst rejection, permeate flux of 65.1 L h^{-1} m^{-2} (vacuum 0.133 bar)	Pressurized system: inadequacy of the membrane Membrane fouling Depressurized system: inadequacy of the membrane	[16]
TiO_2-P25	Susp	SPMR UF	UV	33 trace organic contaminants	For 18 compounds >95% removal For 14 compounds 50%-88% removal For 1 compound no degradation	The presence of organic matter into the aqueous matrix affect the photodegradation efficiency	[79]
TiO_2-P25	Susp	SPMR UF	UV	DCF	Long term operation (72 hours) at 15 L h^{-1} m^{-2} constant permeate flux. With Ultrapure Water matrix: 99.5% DCF degradation; 66% TOC mineralization. Practically constant TMP (-0.14 bar), regardless of the water matrix, thanks to the developed back-flushing protocol (1 min backwashing after 9 min filtration)	Feed-water characteristics influence the photocatalytic efficiency: organic species compete with the drug, inorganic ions act as hole scavenger.	[80]
TiO_2-P25 Lab made TiO_2 GO doped TiO_2	Imm	UF	UV Visible	DPH	GO doped TiO_2 73% degr., 35% miner. (UV) 28% degr., 19% miner. (Visible) 90 and 81 L m^{-2} h^{-1} permeate flux under UV and visible light	Dead end filtration mode NaCl leads to a slight decrease in drug degradation Suspended photocatalyst shows higher photocatalytic efficiency	[52]

TiO_2	Imm	MF	UV-A sunlamp	MB DCF IBU	Hydrophilic TiO_2/PVDF (120 min) 100% MB degr.; 50% IBU degr.; 55% DCF degr. The adsorption properties of the Photocatalytic Membranes were predominant Membrane reusability	Dead end filtration mode Incomplete drug degradation No data on flux and membrane fouling during pollutant photodegradation	[81]
TiO_2 nanotubes	Imm	MF	UV	DCF	TiO_2 nanotubes stability on the membrane 94% DCF degr. (240 min, static tests) 100% DCF degr. (18 days, dead-end tests)	Degradation rate constant with the dead-end flow mode 100 times lower when compared with the static experiment ($0.085 \cdot 10^{-3}$ vs. $9.96 \cdot 10^{-3}$ min^{-1}): the experimental setup of the dead end experiment needs to be optimized	[82]
TiO_2 Nanofiber (NF)	Imm	SSF	UV	CMD	89% drug degr. at 10 L m^2 permeate flux the photocatalytic efficacy of SSFs was inversely proportional to permeation flux because of decreased contact time	Dead end filtration mode Low drug degradation at higher permeate flux (64% and 47% at 20 and 50 L h^{-1} m^{-2}) 3-8% weight TiO_2 NFs loss after sonication (40 kHz) treatment for 30 min	[63]
TiO_2-P25	Susp	DCMD		IBU	100% and 99.4% IBU degr., 95.8 and 94.0 % IBU miner. after 5 hours by operating in batch and continuous mode, respectively. 100% IBU removal	Energy consumption	[83]
TiO_2-P25	Susp	DCMD		DCF	100% DCF degr, 82.5-100% drug miner. depending on initial drug concentration	Energy consumption	[23]
TiO_2-P25	Susp	DCMD		DCF, IBU NAP	Primary effluent: 100% DCF degr., 73% IBU degr., 90% NAP degr., miner < 14% Secondary effluent: 100% DCF degr., 93% IBU degr., 94% NAP degr., miner < 23%	Owing to membrane fouling, primary effluent should be pre-treated. Energy consumption	[84]

(*) GO: Graphene Oxide; (**) susp: suspended; imm: immobilized. (***) LIN: Lincomycin; FUR: Furosemide; RAN: Ranitidine; .GEM: Gemfibrozil, TAM: Tamoxifene; DCF: Diclofenac; IBU: Ibuprofen; DPH: Diphenhydramine; MB: Methylene Blue; CMD: Cimetidine; NAP: Naproxen.

SPMR: Submerged Photocatalytic Membrane Reactor; SSF: Stainless Steel Filter; DCMD: Direct Contact Membrane Distillation.

2.2.1. Suspended photocatalyst into slurry type photoreactor

Augugliaro et al. [78] studied the degradation of Lincomycin (LIN) in aqueous suspensions of TiO_2-P25 irradiated by sunlight. The proposed PMR, obtained by coupling the solar PR with catalyst in suspension with a NF membrane module, increased LIN degradation with respect to the slurry PR alone. Rejections of 93.64% and 97.78% were obtained for DK2540C membrane by using an initial concentration of LIN of 25 and 75 μM, respectively. Lower rejections (82.6% and 91.3%) were obtained by using the DL2540C membrane under the same experimental conditions.

The data collected by using the PMR in continuous mode (Fig. 4) indicated that the presence of the membrane allows reducing both the substrate and intermediates down to very low concentration levels in the permeate (open symbols). A TOC accumulation in the system throughout the runs was observed, with an extent depending on solar irradiance and initial lincomycin concentrations. This trend was explained by considering that under the experimental conditions used, the amount of photons entering the system per unit time is not sufficient to mineralise the drug fed in the photoreactor per unit time.

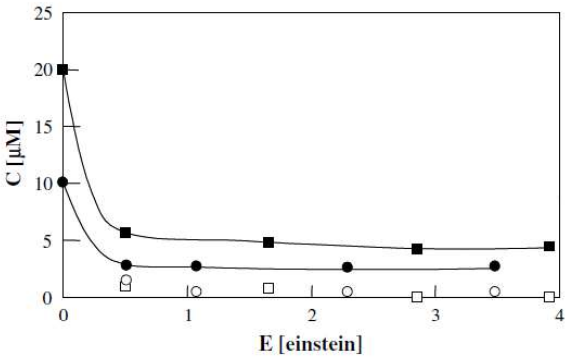

Fig. 4. Lincomycin concentrations versus the cumulative photon energy, E, for runs carried out in continuous regimen by using the PMR. Full symbol: retentate; open symbol: permeate [78].

One year later, Molinari et al. [29] studied the photodegratation of PhACs in a continuous recirculation slurry PMR by using TiO_2-P25 as the catalyst and a laboratory NF unit equipped with different membranes. The influence of operating pH on the degree of adsorption of various PhACs onto the catalyst surface was studied, evidencing the importance of this parameter, affecting the hydrophilic/hydrophobic character of the catalyst. The rejection values obtained in the PMR system by using the NTR 7410 membrane were in the range between 10–60% and 5–30% for furosemide and ranitidine, respectively, in the dark, evidencing that the chosen membrane was

555 not adequate to retain the drug in the reaction environment. No rejection of PhACs was observed
556 during the photodegradation test conducted in the presence of light, photocatalyst and oxygen,
557 showing that the membrane is only able to confine the photocatalyst. These results confirm that
558 the right choice of the membrane is a key step for PMR development.
559 In a successive work the same authors [16] studied the photodegradation of two pharmaceuticals
560 (Gemfibrozil (GEM) and Tamoxifen (TAM)) using suspended TiO_2-P25 as catalyst in pressurized and
561 depressurized PMR configurations. Commercial flat sheet NF membranes NTR 7410 with exposed
562 membrane surface area of 19 cm^2 were used in the photocatalytic tests in the pressurized PMR.
563 Commercial capillary polyethersulfone (PES) membranes, assembled in a module with exposed
564 membrane surface area of 4.19×10^{-3} m^2, were used in the depressurized PMR.
565 In the pressurized system, a good operating stability was observed by operating in continuous
566 mode in the degradation of GEM, reaching a steady state in ca. 120 min, with a complete removal
567 of the drug, 60% mineralization and constant permeate flux of 38.6 L h^{-1} m^{-2} (TMP = 6 bar) that
568 remained constant until the end of a run. A TOC rejection of about 62% at steady state confirmed
569 the need to identify a membrane with higher rejection to the intermediate products. Catalyst
570 deposition on the membrane surface and fouling caused a flux decline during the photocatalytic
571 process. A washing of membranes with an enzymatic detergent was enough to restore the flux at
572 acceptable values.
573 In the case of TAM degradation test the membrane was not able to reject significantly it and its
574 degradation intermediates which were also found in the permeate.
575 The depressurized system, developed to control membrane fouling, was built by changing the
576 pressurized permeation cell with the depressurized permeation system schematized in Fig. 5. The
577 oxidant was fed by means of oxygen bubbling in the permeation module, having the dual purpose
578 previously described [48]. Obtained results evidenced that the membrane retained only the
579 catalyst in the reaction environment, while GEM and its oxidation products moved in the
580 permeate. However, the submerged PMR permitted to obtain a steady-state flux of 65.1 L h^{-1} m^{-2}
581 at a vacuum of 0.133 bars, higher than those obtained operating with the pressurized module,
582 showing it interesting for application purposes, provided a suitable permselective membrane
583 versus the substrate, is used.
584

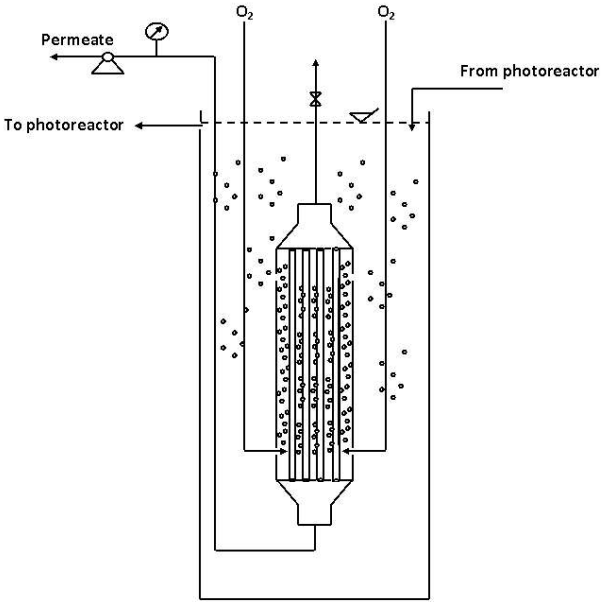

Fig. 5. Scheme of the depressurized permeation cell with submerged membranes [16].

Based on the same approach, Fernandez et al. [79] tested a submerged photocatalytic membrane reactor (SPMR) with air bubbling in the photocatalytic degradation and removal of 33 trace organic contaminants (TrOCs), including drugs, analgesics, antibiotics, surfactants or herbicides, from aqueous media. Obtained results showed that there was a group of 18 compounds that were completely degraded (>95% removal). Another group of 14 compounds showed removal percentages in the range 50%-88%. The last compound, which is a flame retardant tris(2-chloroethyl) phosphate (TCEP), was not degraded from photocatalysis. It was found that these results were strictly correlated with the kinetic of photodegradation of those compounds. In particular all compounds having kinetic constant (k) values higher than 0.0544 min^{-1} were effectively removed in the PMR with an extent following the same trend of k value.

In running some membrane plants a practical requirement is operating at constant permeate flow rate, thus continuously treating a constant feed flow rate. In that case, usually TMP is progressively increased to compensate the increase of membrane resistance due to membrane fouling, till reaching a limit of TMP. Sarasidis et al. [80] demonstrated that an appropriate membrane back-flushing protocol can avoid this trend. The performance of a laboratory pilot SPMR operating in continuous mode in the degradation of Diclofenac (DCF) was evaluated. The submerged UF membrane module consisted of 136 hollow fibers with a total surface area of 0.097 m^2. It was operated under constant permeate flux (15 L m^{-2} h^{-1}), with air bubbling and periodic membrane back-flushing. Long-term continuous experiments lasting three days were carried out. The operating pH showed an important influence on system performances. At steady state

conditions, which was reached after about 1-2 hours, pH = 6 and TiO_2 = 0.5 g L^{-1}, DCF degradation and TOC mineralization was 99.5% and 66%, respectively, while no loss of TiO_2 particles into the permeate was recorded. The observed incomplete mineralization may be attributed to the formation of degradation products that are recalcitrant to further decomposition. The PMR system was submitted to an automatic periodic membrane backwashing (1 min backwashing after 9 min filtration), which effectively controlled membrane fouling, thus permitting stable continuous operation. Indeed the operating TMP remained practically constant during the 72 hour of operation at constant permeate flux.

Since water quality can strongly affect the performance of TiO_2 photocatalytic process [85], both Fernandez et al. [79] and Sarasidis et al. [80] studied the influence of water matrix on the performance of photocatalytic degradation and removal in PMR. Fernandez et al [79] carried out some experiment with the 33 TrOCs dissolved in an organic-based model water solution containing humic acids (HA), bovine serum albumin (BSA) and low viscosity sodium alginate (NaA), providing a final TOC concentration of 5.6 mg L^{-1}. The results showed that the presence of organic matter within the feed matrix generally caused a decrease in the removal efficiency. Sarasidis et al. [80], considering ultrapure water (UW), tap water (TW), and groundwater (GW) also found significant differences, evidencing the important role of feed-water characteristics (i.e. presence of organic and inorganic scavengers) on process effectiveness. The TMP remained practically constant during the long-term continuous operation of the PMR system (72 h), regardless of the water type, confirming the effectiveness of the developed automatic backwashing protocol.

The observed decreased removal efficiency in the presence of other organic and inorganic species in the aqueous matrix was caused by various phenomena. In particular, the additional organic species present in the natural water matrices may compete with drug or other molecules to be degraded for active TiO_2 surfaces and OH• attack and may contribute to light attenuation in the photoreactor. Moreover, the presence of specific inorganic ions may result in a partial deactivation of the TiO_2 nanoparticles. Ions as Cl^-, HCO_3^-, NO_3^- and SO_4^{2-} detected in groundwater and tap water, can act as hole scavenger, competing with the production of OH• radicals. These findings highlight the need for good knowledge of feed water properties to successfully design a PMR treatment process for effectively removing organic micropollutant from aqueous media.

Summarizing, these results confirm that PMRs can be of interest in the removal of PhACs from water because they allow the recovery and reuse of the catalyst, permit to achieve a continuous process and, if a suitable membrane is found, it is possible to retain the pollutant and its

degradation products in the reaction environment. The operating pH is an important parameter in the heterogeneous photocatalytic process, as it may affect i) the surface charge of the photocatalyst and then its interaction with the substrate and ii) the size of catalyst aggregates as well as the positions of conductance and valence bands. So it must be to appropriately selected. The need to study strategies to avoid membrane fouling caused by the use of pressure as driving force, as reported in the case of dyes abatement, is also confirmed. Submerged membrane with air/oxygen bubbling and the development of an appropriate backwashing protocol represents an interesting approach to limit this problem.

2.2.2. Entrapped photocatalyst into photocatalytic membrane

In comparison with the works published on the study of PMs for removal of organics like textile dyes, only few studies are available on use of this technique for remediation of PhACs.

In their work Pastrana-Martinez et al. [52] also considered the photocatalytic degradation of a pharmaceutical compound, diphenhydramine (DPH). Obtained results evidenced that the M-GOT and M-P25 are very active PM, presenting comparable efficiencies under UV-Vis irradiation in terms of DPH removal during the first photocatalytic cycle (ca. 73% in DW and ca. 60% in SBW). A lower DPH removal was obtained by using the M-TiO_2 PM (43% in DW and 39% in SBW). Concerning to the visible irradiation, as observed in the case of the dye MO, the M-GOT system was the best one, with a photocatalytic degradation of ca. 28%. TiO_2 based membranes (M-P25 and M-TiO_2), showed a very low activity (ca. 5%) since TiO_2 is not active under visible irradiation, while the addition of GO, decreasing the band gap, promote the visible light activity. Also in this case the presence of NaCl (0.5 g L^{-1}) leads to a slight decrease in DPH degradation since Cl^- ions acted as holes and hydroxyl radical scavengers.

As previously reported, an important aspect to take into consideration when preparing PMs, is represented by the necessity to obtain an effective dispersion of the catalyst particle into the membrane, thus limiting the intrinsic limitation of such systems. Some preparation methods (e.g. dip coating) usually result in the formation of nanoparticles agglomerates on the membrane, having an important effect on membrane activity reduction [86, 87]. Fisher et al. [81] proposed a new and straightforward method for preparing photoactive MF membranes by direct synthesis of TiO_2 nanoparticles on the surface of two hydrophilic membranes (PES, PVDF) and one hydrophobic membrane (PVDF) by hydrolysis of titanium tetraisopropoxide (TTIP). To do this, a wet (water) membrane was dipped in a TTIP/ethanol solution. As the water film on the membrane surface

initiates the hydrolysis, TiO_2 nanoparticles grown on the membrane surface. Operating in this way a layer of non-aggregated TiO_2 nanoparticles strongly bounded to the membrane surface was directly built on site.

The fouling behavior of the membrane was evaluated by cyclic permeation tests of BSA solution. Obtained results showed improved fouling resistance of the hydrophilic TiO_2/PVDF membrane compared with the untreated membranes.

The three PMs were tested in the photodegradation of methylene blue (MB), ibuprofen (IBU) and diclofenac (DCF). Obtained results are summarized in Table 5 in terms of pollutant degradation after 120 min of photodegradation. In the case of MB better performance was obtained by using the hydrophilic TiO_2/PVDF, despite the lower TiO_2 content with respect to the TiO_2/PES (see Table 5), because of the higher rate of adsorption indicating an higher affinity of the membrane towards MB. The hydrophobic PVDF modified membrane was the worst, because of the lower contact with water dissolved MB. Then the adsorption properties were most determinant than the TiO_2 content. Lower degradation rates were obtained by degrading DCF and IBU, because of the higher amount contained in water, resulting in high drug concentration in the treated water. Two or more permeate recycle were need to obtain acceptable permeate quality, as observed by Athanasekou et al [50] in the case of dyes. No fouling studies during photodegradation tests were reported.

The TiO_2/PES membrane was reusable, as demonstrated during 5 successive cycles of complete degradation of MB. The photocatalytic activity was fully maintained and no damage of the polymeric support happened, since the TiO_2 layer totally covers the support acting as a protector from UV light [88].

Table 5: Pollutant degradation after 120 minutes of tests for the three different membranes (initial concentrations: MB = 3.2 mg L^{-1}; DCF = 25 mg L^{-1}; IBU = 100 mg L^{-1}) [81]

Photocatalytic Membrane	TiO_2 content (%)	Degradation (%)		
		MB	IBU	DCF
TiO_2/PES	0.809	70	44	68
Hydrophilic TiO_2/PVDF	0.092	100	50	55
Hydrophobic TiO_2/PVDF	0.345	15	/	/

The use of TiO_2 nanotubes is also expected to be a promising solution to overcome the intrinsic drawbacks of PMs, because of their high surface-area-to-volume ratio, short distance for charge carrier diffusion and high photon-collection efficiency [89, 90]. On this basis, Fisher et al [82] also proposed the preparation of nanotubular TiO_2–PES membranes, obtained by an appropriate procedure of assembly and crystallization of TiO_2 nanotubes on the membrane, and tested the prepared membrane in the degradation of DCF under UV light. A complete TiO_2 nanotubes stability on the PES membrane was found. During static photodegradation tests, a 94% DCF degradation (initial concentration of 5 mg L^{-1}) was obtained after 240 min, while by operating in dead-end flow mode, a 100% DCF degradation was obtained after 18 days, evidencing a lower degradation rate constant when compared with the static experiment ($0.085 \cdot 10^{-3}$ vs. $9.96 \cdot 10^{-3}$ min^{-1}). This considerable difference was due to the different surface of membranes and volume of the solution to be treated, as well as to the consideration that only 20% of the solution was irradiated during the cross-flow tests, leaving 80% unused in the flask and tubes. Then, in order to yield higher degradation rates, the experimental setup of the dead end experiment needs to be optimized.

Another interesting approach to overcome the intrinsic limitation of PMs consists in developing nanofiber based PMs. Indeed, as previously reported, among various physical forms (e.g. film, particle, etc.) TiO_2 nanofiber has lower self-agglomeration tendency and can provide a larger effective (i.e. photoactive) surface. On this topic, Ramasundaram et al. [63] prepared and tested TiO_2 nanofibers (TiO_2-NFs) integrated stainless steel filter (SSF) in the photodegradation of the drug cimetidine (CMD). The photoactive SSF was prepared by the following steps (see Fig. 6): i) preparation of a free-standing TiO_2-NFs layer by the electro spinning technique; ii) bonding of this TiO_2-NFs layer to SSF surface through a hot pressing process with a PVDF-NFs interlayer as a binder.

The thickness of the binding layer influences both the stability and the photocatalytic activity of the prepared photocatalytic SSFs. The stability was determined by covering the SSF with five different thicknesses of PVDF-NFs layer (12, 22, 32, 42, and 64 μm). These samples were immersed in water, subjected to sonication (40 kHz) treatment for 30 min. The percentage of weight loss after sonication were 5, 8, 3, 1, and 4 wt.%, respectively. Then, 42 μm thickness was the optimum for binding TiO_2-NFs firmly to the surface of SSF.

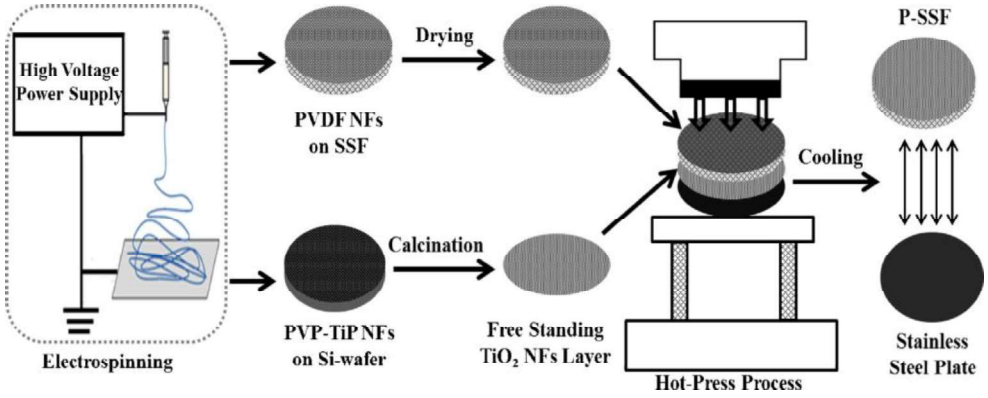

Fig. 6. Overall preparation process followed to integrate TiO_2 NFs on SSF using PVDF binder layer [63]

Photocatalytic tests were carried out in dead-end filtration mode. When the thickness of TiO_2-NFs increased from 10 to 29 μm, the photodegradation of CMD increased from 42% to 90%. A further increase of the thickness of the TiO_2-NFs layer did not had significant effect on drug degradation, probably caused by limited light penetration.

The photocatalytic efficiency of the photocatalytic SSFs varied also by changing water flux. CMD photodegradation were found to be 89%, 64%, and 47% at flux conditions of 10, 20 and 50 L h^{-1} m^{-2}, respectively, indicating that photocatalytic efficacy of the photocatalytic SSFs toward the oxidation of CMD was inversely proportional to permeation flux. This trend was ascribed to the reduction in contact time between the drug molecules and TiO_2 layer when the flux increases.

2.2.3. Coupling of photocatalysis and membrane distillation

In 2012 Mozia et al. [83] used their hybrid photocatalysis–DCMD system for removal of ibuprofen (IBU) from tap water. IBU photodegradation of ca. 91.5% and 100% were obtained after 1 h and 5 h of the process, respectively, by operating in batch mode, and ca. 80% and 99.4% in continuous mode. The distillate did not contain IBU in both the operating modes, corresponding to a 100% IBU removal. TOC in the distillate after 5 h was approximately 1.1 mg and 1.6 mg, for continuous and batch mode, respectively. Then the influence of the operation mode on the quality of the treated water and on drug mineralization was not significant. Because of the higher potential for large scale application, the coupled PMR/DCMD system, operated in the continuous flow mode, is recommendable.

Membrane fouling in the PMR/DCMD during long term process (315 h) operating in continuous was also studied, by monitoring the distillate flux. The results, summarized in Fig. 7, evidence an

increase of distillate flux decline during the experiments. After 54 h the flux decreased for ca. 7% compared to pure water flux (272 L m^{-2} d^{-1} vs. 294 L m^{-2} d^{-1}), whereas after 188 h a flux of 41 L m^{-2} d^{-1} was detected, corresponding to an 86% flux decline. This trend was caused by a deposit layer (calcite and aragonite crystals) formed on the membrane surface. A cleaning with HCl solution allowed to dissolve the $CaCO_3$ scale deposit and to recover the flux. However, about 70 h after washing with HCl solution, the flux started decreasing with a similar trend as before cleaning.

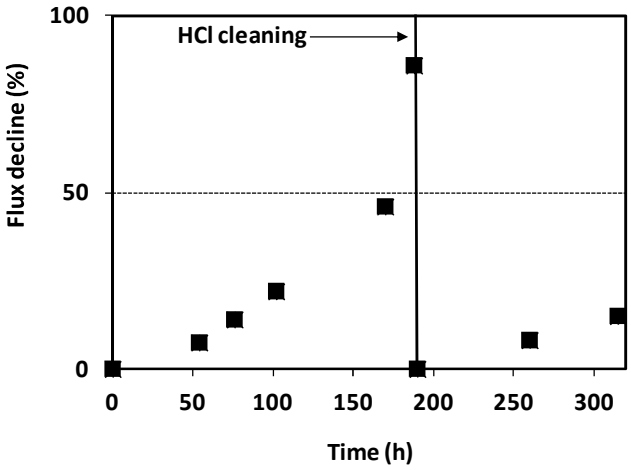

Fig. 7. Distillate flux decline versus the time during long term operation of PMR/DCMD in continuous mode (data from [83]).

In a successive work the same authors [23] applied the PMR/DCMD system in the removal of diclofenac (DCF) from water, obtaining similar results in terms of DCF decomposition (ca. 100%) and mineralization, with values in the range 82.5–100% depending on initial drug concentration, being the highest for the lowest DCF concentration. The distillate did not contain DCF as well as its photodegradation products (TOC ca. 0.8 mg/L), confirming the effectiveness of membrane distillation in obtaining a distillate of optimal quality, higher than that one obtained by coupling photocatalysis with pressure driven membrane processes.

Since, as previously reported, the water quality strongly affects the performance of TiO_2 based photocatalytic process, the same approach (PMR/DCMD) was tested [84] in the removal of a mixture of diclofenac (DCF), ibuprofen (IBU) and naproxen (NAP) sodium salts from different aqueous matrices: ultrapure water (UW), tap water (TW), primary effluents (PEs) and secondary effluents (SEs) of municipal wastewater treatment plant. When PEs were used as feed, DCF was removed completely, IBU amount decreased for 73% and NAP for 90%. In the case of SEs, DCF, IBU

779 and NAP concentrations decreased by 100%, 93% and 94%, respectively. Mineralization did not
780 exceed 14% for PEs and 23% for SEs. No drugs were found in the distillate. Thus the hybrid
781 PMR/DCMD system can be an effective technology for the removal of PhACs from SE and PE.
782 Nevertheless, owing to membrane fouling, the latter should be pre-treated before to be fed in the
783 hybrid system.
784 Summarizing, the results obtained by Mozia et al. [23, 83, 84] by applying the PMR/DCMD system
785 confirmed that this system represents a promising method also for treatment of waters containing
786 PhACs. MD separates efficiently both TiO_2 particles and organic contaminants present in feed
787 solution and presents lower fouling problem compared to pressure driven membrane processes.
788 The relatively low distillate flux, which represents a limit in the case of dye, considering that drugs
789 are a more recalcitrant class of organic pollutants, assured the required residence time of
790 contaminants in the photoreactor thus giving high photodegradation efficiency. The high energetic
791 consumption of MD represents an important cost item to be considered when comparing
792 PMR/DCMD process with PMR/UF or PMR/NF, also considering the high quality of membrane
793 distillate and the lower MD fouling.
794
795 **2.3. Comparison between PMR application in the photodegradation of dyes and**
796 **pharmaceuticals in aqueous media**
797 The results described in the previous sections clearly demonstrate that PMRs were successfully
798 applied in the photodegradation of both dyes and PhACs contained in aqueous media, both in the
799 case of suspended and immobilized TiO_2.
800 The difficulties encountered in developing efficient PMRs are similar, regardless the type of
801 organic pollutant. In the case of slurry configuration of PMRs, particular attention has to be
802 devoted to prevent membrane fouling, which causes a decrease of membrane permeability and
803 accumulation of the photocatalyst nanoparticles on the membrane surface. Also light scattering by
804 catalyst particles and dissolved organics has to be considered. Besides it is important to have good
805 knowledge of feed water properties, because they affect PMR performance. The use of SPMRs
806 with air bubbling and adequate membrane back-flushing represents an interesting approach to
807 minimize these difficulties.
808 In the case of photocatalytic membranes, the moderate loss of photoactivity, the possible
809 membrane photodegradation because of direct light irradiation, the mass transfer limitations and
810 the possible catalyst deactivation and wash out represent factors to be appropriately considered.

The preparation of PMs, with opportune porosity and pore size and effective dispersion of the catalyst particles, represents a solution to previous drawbacks.

The same parallelism was observed in the case of DCMD/photocatalysis hybrid system.

The implementation of a PMR system is not significantly influenced by the type of pollutant considered, while it is fundamental to consider the intrinsic limitation of the chosen PMR configuration. Another difference is related to the recalcitrant character of the organic pollutants to be degraded: higher the recalcitrant character, higher the required residence time of contaminants in the photoreactor and/or the contact time with the photocatalyst to give satisfactory photodegradation efficiency. On our point of view, SPMRs can have, at present, greater perspective of industrial applications. Indeed, use of commercial membranes suitable also for non photocatalytic applications and possibility to separate the reaction zone and the separation zone are two important design aspects.

2.4. Submerged photocatalytic membrane reactor (SPMR) for removal of other organic pollutants

Natural organic matter (NOM) is widely distributed in soil, natural water, and sediments and consists of a mixture of the decomposition products of plant and animal residues [91]. Fulvic acid (FA) represents more than 70% of NOM in surface waters [92]. Consequently control of FA is important in treating the surface water.

As evidenced in the previous sections, the major problems in PMRs, coupling slurry type photoreactors and pressure driven membrane processes, are related membrane fouling, which is emphasized when treating natural waters, because of the presence of dissolved NOM. On this basis, Fu et al [57] studied the photodegradation of FA by using synthesized nanostructured TiO_2/silica gel photocatalyst particles in the SPMR schematized in Fig. 8.

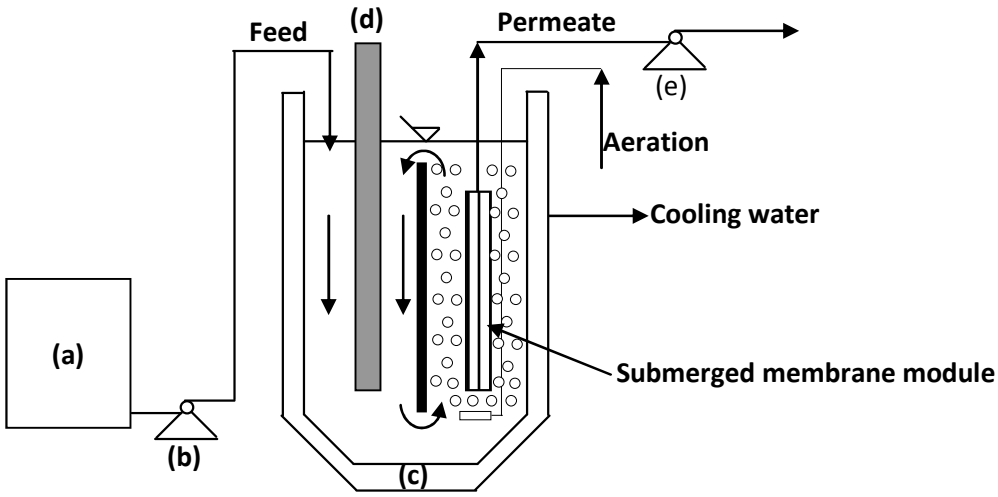

Fig. 8. Schematic diagram of the SMPR system: (a) feed tank; (b) feed pump; (c) thermostated jacket photoreactor; (d) UV lamp; (e) suction pump (elaborated from [57]).

The optimal conditions for FA removal were 0.5 g L^{-1} photocatalyst concentration, 0.06 m^3 h^{-1} airflow and acidic conditions.

An increase of permeate flux was observed by using nano-structured TiO_2 instead of bare TiO_2 P25 powder, evidencing that the use of nano-structured TiO_2 resulted in reduction of fouling problems. A similar approach was applied by Zheng et al. [93] for virus removal from aqueous media. They used the experimental set-up schematized in Fig. 9, operated under constant flux mode. Bacteriophage f2 (mean size of 25 ± 1 nm), which is similar in size to the human enteric virus, was used as the model virus. Nano-TiO_2 P25 was used as the photocatalyst. The influences of filtration flux and permeation mode (continuous or intermittent) were tested.

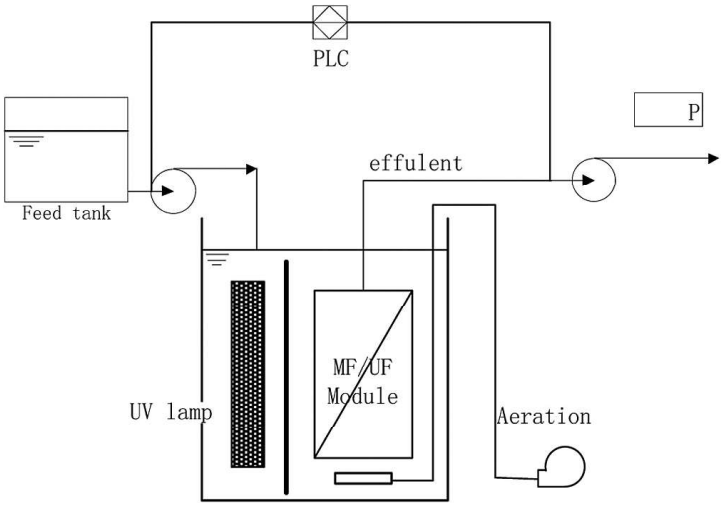

Fig. 9: Schematization of the SPMR employed by Zheng et al. [93] (reactor total volume = 12.75 L; 4 W UV-C (254 nm) lamp; flat-sheet PVDF membrane (pore size 0.15 μm, membrane area 0.03 m^2); aeration rate 10 L min^{-1}; PLC: control system; feed temperature 20–25 °C).

The optimal operating condition was determined to be the intermittent suction mode with a filtration flux of 40 L m^{-2} h^{-1}. Above this value irreversible fouling was observed, as reported also by Kertèsz et al. [48] in their system. 99.999 % virus removal on average after 24 h of continuous operation was obtained, evidencing that the SPMR permitted virus inactivation thanks to the action of OH• and to the membrane, which acted as a barrier for both photocatalyst and virus. Summarizing, the results obtained by Fu et al. [57] and Zheng et al. [93] demonstrated that a SPMR, operated with fine-bubble aeration and membrane backflushing, is able to remove different organic pollutants from waters limiting the problems related to membrane fouling.

2.5. Coupling of photocatalysis with dialysis

Starting from the main limit of the MD/photocatalysis hybrid system proposed by Mozia et al. [23, 55, 56, 83, 84] that is the significant energy requirement to reach evaporation, Azrague et al. [94] proposed the combination dialysis/photocatalysis to mineralize organic compounds contained in artificial turbid waters obtained by using bentonite.

The dialysis membrane, separating the polluted turbid water compartment from the photocatalytic compartment, acts as barrier for the photocatalyst particles and allows to extract the organic compounds (2,4-dihydroxybenzoic acid (2,4-DHBA) in this study) from the turbid water thanks to the concentration difference between the two compartments. The absence of TMP avoids fouling. Besides, the membrane permits: i) to maintain the TiO_2 in the photocatalytic

compartment avoiding a final filtration stage, and ii) to keep the bentonite away from the photoreactor, thus avoiding the light scattering from bentonite particles. Another aspect to be remarked is that the membrane module is not irradiated, so that the membrane cannot be degraded in any way. These advantages, combined with the complete removal of 2,4-DHBA, demonstrate the effectiveness of the proposed PMR combining photocatalysis and dialysis. The design of a PMR working in a continuous mode should be also possible.

2.6. Coupling of photocatalysis with pervaporation

In 2007 Camera-Roda and Santarelli [95] tested the integration of photocatalysis with pervaporation (PV), demonstrating that such an approach permits to improve the efficiency of the detoxification of water streams containing recalcitrant organic pollutants (as 4-chlorophenol (4-CP) used as model pollutant) at a low concentration.

In PV, separation is based on the relative volatility of the components in the mixture and also depends on the relative affinity of the components with the solid matrix of the membrane. Thus the choice of membrane material is important to obtain a selective separation of the molecules.

In the experimental set-up utilized, a diaphragm pump continuously recycled the water to be treated to an Annular Photocatalytic Reactor (APR). At the exit of the APR, the water fed one or two plane PV modules containing organophilic membranes (membrane surface area = 160 cm^2) through which the organic components permeate selectively, thanks to the vacuum (6 mbar) that is kept downstream. The retentate comes back in the photoreactor. The temperature is kept constant and oxygen is continuously supplied inside the photoreactor maintaining a constant concentration of 8 mg L^{-1} in the system.

The results, summarized in Fig. 10, show that the rate of disappearance of 4-CP is highly improved by using the integrated system thanks to the synergy between photocatalysis (PC) and PV resulting in a process intensification. Practically PV positively influences PC as the membrane continuously removes some intermediate products that could slow down the rate of the photocatalytic reaction. Concurrently, the PV step takes advantage from the PC since the latter transforms the weakly permeable 4-CP into organic compounds that PV can remove at a high rate, i.e. hydroquinone and especially benzoquinone. In the figure the curve “PC+PV, no integration” represents the arithmetic sum at each time of the removals given by PC and PV acting alone. This curve represents the degradation of the two processes in the case they would operate in series, without integration, and is always higher than the curve representing the integrated process,

908 because it does not consider the synergistic effect. Thus the synergy between PC and PV is
909 demonstrated.
910

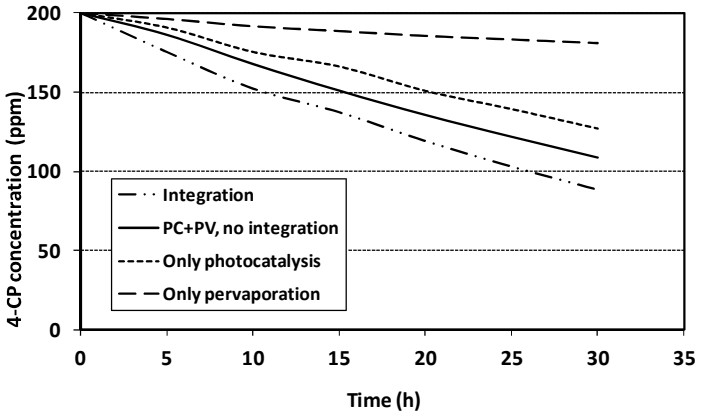

911
912 **Fig. 10.** 4-chlorophenol (4-CP) concentration versus time in the integrated photocatalysis-PV
913 process (data from [95]).
914
915 Process intensification by synergistic effect depends on the optimization of the ratio between the
916 characteristic rates of the PC and PV processes. To maximize the synergistic effect, the rates of the
917 two processes should be balanced, as if one of the two has a characteristic rate much higher than
918 that of the other one, then only the latter can significantly benefit of the integration.
919 This approach, despite the above mentioned results, possesses the following significant
920 drawbacks: i) the concentration of 4-CP in the retentate after 30 hours of the hybrid process is
921 equal to ca. 50% of the initial one, resulting in ca. 50% 4-CP degradation; ii) the photodegradation
922 intermediates, i.e. hydroquinone and especially benzoquinone, are removed at a high rate by PV,
923 resulting in unsatisfactory mineralization; iii) the permeate solution, containing this by-product,
924 need to be opportunely treated.
925
926 **3. Photocatalytic membrane reactors in the synthesis of organic substances**
927 Traditional industrial processes employed for the synthesis of organic substances are becoming
928 even more unsustainable in terms of resources and environmental impact [5, 13, 14, 96, 97].
929 On the basis of this, the application of photocatalytic reactions to organic synthesis has attracted
930 high interests to develop, in perspective, environmentally benign synthetic processes [10].
931 Heterogeneous photocatalysis, based on the use of a solid semiconductor, is a discipline that
932 includes a large variety of reactions. Among them reduction and oxidation processes play an

important role in the production of a wide range of chemicals and precursors in the synthesis of organic compounds with high added value such as drugs, vitamins, fragrances, etc.

Despite the great potentiality of the photocatalytic process and the important advantages that can be achieved by its coupling with a membrane separation system, to the best of our knowledge there are no photocatalytic synthesis of organic compounds such as oxidation or reduction reactions coupled with PMRs beyond those that will be presented in this review.

One example of oxidation reaction carried out in PMR is the one-step conversion of benzene to phenol showing the possibility to use a photocatalytic reaction coupled to product separation by means of a membrane contactor [4]. The choice of a membrane permeable to phenol is crucial because it is more reactive than benzene and its permeation from the reacting solution avoids its oxidative degradation. The same general approach has been used in the partial oxidation of ferulic acid to vanillin (VA) [98]. In this case the utilization of a highly selective PV membrane allows the continuous recovery of VA by PV. One of the first examples of reduction reaction carried out in PMR is the hydrogenation of acetophenone to produce phenylethanol, a compound of wide industrial interest [99]. It was found that use of a membrane reactor improves the efficiency of the photocatalytic reaction compared to a batch reactor thanks to the extraction of phenylethanol in the organic extracting phase. Common benefits of the above integrated processes are the complete retention of the photocatalytic powder in the reacting medium, high degree of purification of the product simultaneously to the reaction, thus enhancing the productivity, yield and selectivity.

In these systems, the choice of the membrane module configuration is mainly determined by the type of photocatalytic reaction and the membrane can assume many roles, as catalyst recovery, separation of the products, rejection of the substrate, etc. Besides, when the photocatalytic process is used as a synthetic pathway the use of an appropriate membrane [100, 101] can allow the selective separation of the product minimizing its degradation. Although these potentialities, the research in the field of PMRs remains still low for photocatalytic reduction.

In the following the above mentioned processes will be described and discussed with greater details.

3.1 PMR in partial oxidation: Conversion of Benzene to Phenol

The one-step synthesis of phenol is of industrial interest. It is an important intermediate for the synthesis of petrochemicals, agrochemicals, and plastics with high production on a worldwide

basis [102, 103]. Today, most of the worldwide phenol production is based on the "cumene process" but this has some disadvantages such as: high and damaging ecological impact, an explosive intermediate to manage (cumene hydroperoxide), large amount of acetone as by-product and a multistep character, making it difficult to achieve high phenol yield compared to benzene [104, 105].

The search for new routes for phenol production based on the one-step direct benzene oxidation became more intensive in the last decade. Among the various routes, the photocatalytic approach is very interesting because it is a "green process" where light and a photocatalyst are used to generate OH• radicals to oxidize benzene. ''Green'' characteristics make photocatalysis an attractive process, such as use of safer catalysts, e.g. TiO_2 which is a component of pharmaceuticals and toothpastes; use of mild oxidants (molecular oxygen); possibility to work in mild conditions running reactions closer to room temperature and pressure; request of very few auxiliary additives; no production of harmful chemicals. However this reaction is little selective because phenol is more reactive than benzene and by-products can be formed [106-115]. To limit this problem, the use of Photocatalytic Membrane Contactor (PMC), that permits the combination of membrane separation and photocatalytic reaction in one device, reduces the formation of by-products. Indeed, the main advantage in using a membrane in this system is the separation of phenol from the reaction mixture permitting to obtain improvements of yield and selectivity limiting side catalytic reactions. On the basis of this Molinari et al. 2009 [4] studied the direct benzene conversion to phenol in a hybrid photocatalytic membrane reactor using TiO_2 as suspended catalyst. In this system the simultaneous phenol separation is performed by using benzene as both reactant and extraction solvent and a polypropylene membrane to separate the organic phase from the aqueous environment. The reaction performed is the following:

$$C_6H_6 + \frac{1}{2}\,O_2 \xrightarrow{hv} C_6H_5OH \qquad (3)$$

Preliminary experimental tests to study the effect of different parameters on this reaction showed that the phenol production did not depend on the unsolved substrate but from the little solubilised amount, evidencing the need to use a system that provides continuously benzene in order to maintain a constant concentration in the aqueous ambient (the biphasic membrane contactor). The photocatalytic reaction rate depends on the catalyst concentration, as shown in Fig. 11. Increasing the catalyst concentration the reaction rates increase although with a

concentration of 1.0 g L^{-1} a quick degradation of phenol is observed after 180 minutes. Thus it is preferable to use a lower catalyst concentration and this limits also the fouling phenomena.

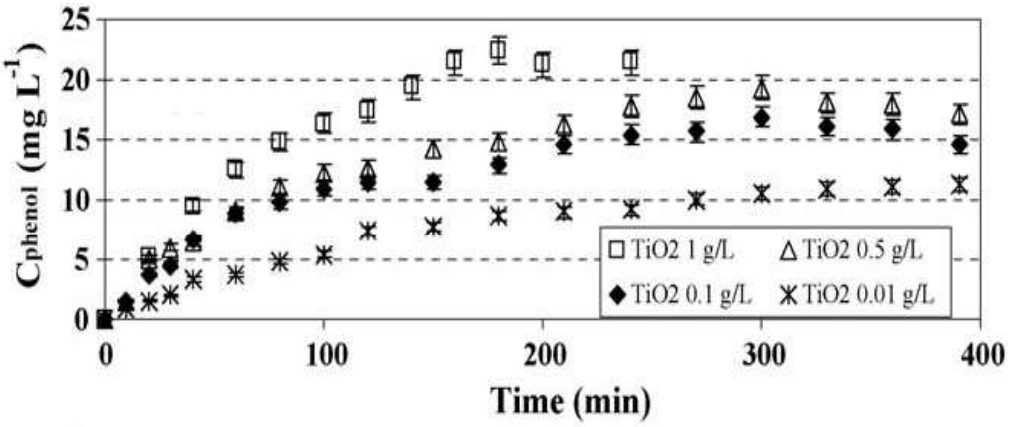

Fig. 11. Phenol concentrations versus the time at different catalyst amount (pH = 5.5, Intensity = 6.0 mW cm^{-2}, T = 25 °C) [4].

Alkaline pH allowed to obtain a higher phenol concentration (20.2 vs 15.0 ± 0.5 mg L^{-1} in acidic conditions) caused by a lower phenol adsorption on the catalyst surface which reduced its degradation. Indeed at alkaline pH both TiO_2 and phenol (dissociated as phenolate) are negatively charged.

To verify the efficiency in terms of flux and extraction degree of phenol in the organic phase, extraction and transport tests were carried out. Obtained results (Fig. 12) showed that use of benzene as organic phase in the role of solvent (other than substrate) allowed the separation of phenol from the aqueous ambient with a partition coefficient (K_D) which reached a value of 2.1, providing also a constant restocking of substrate (about 200 mg L^{-1}) in the aqueous phase.

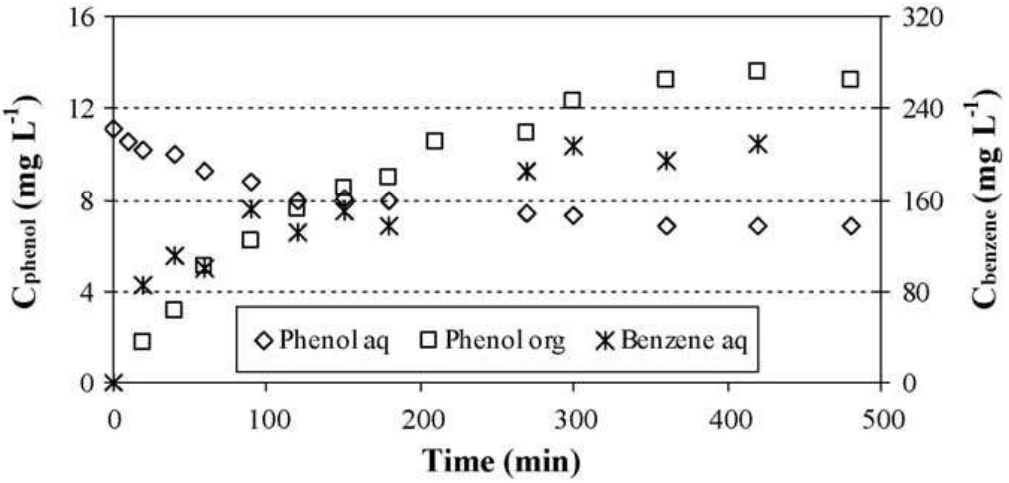

Fig. 12. Phenol concentration in aqueous and organic phases and benzene concentration in the aqueous phase during the transport tests without photocatalysis (initial phenol concentration in the aqueous phase 10 mg L^{-1}) [4].

On the basis of the obtained results, a PMR set-up was built (Fig. 13) by connecting a photocatalytic section with a separation zone by means of a peristaltic pump (4). The photocatalytic section was constituted by a batch reactor (2) containing the aqueous acidic solution with the catalyst (TiO_2) in suspension, equipped with a Pyrex glass jacket surrounding it which allowed to maintain the system at a temperature of 25 °C. Above the reactor a 500 W medium pressure Hg lamp (3) (light intensity = 6.0 mW cm^{-2}, UV-vis range: 240-440 nm, maximum emission at λ= 366 nm) was placed. The separation zone consisted of a biphasic membrane contactor immersed in a thermostatic bath (5). It was constituted by two compartment cells (V = 130 mL) separated by a hydrophobic flat sheet polypropylene membrane with an exposed surface area of 28.3 cm^2. The first compartment (6) contained the aqueous reactive phase coming from the photoreactor. The second compartment (7) contained an organic phase (only benzene) mechanically stirred by a motor, acting both as stripping solution and reagent.

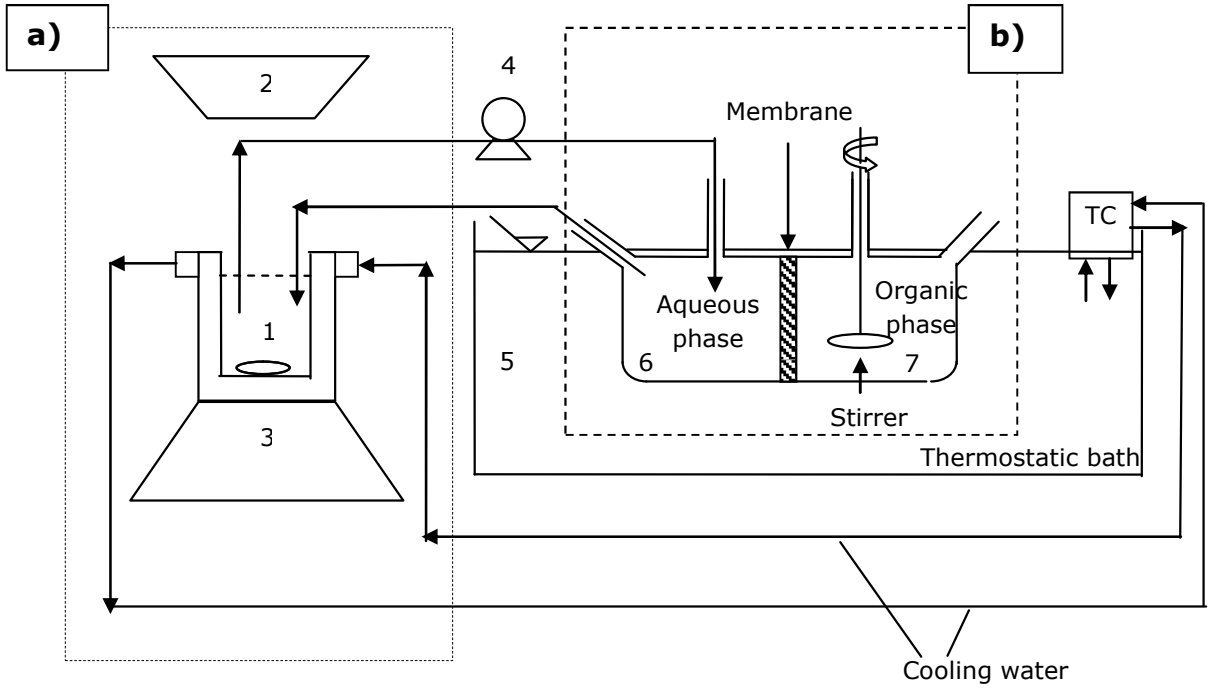

Fig. 13. Scheme of the experimental set-up: photocatalytic reactor (a) coupled with the membrane contactor (b) (1: batch reactor, 2: UV lamp, 3: magnetic stirrer, 4: peristaltic pump) [4].

In this system benzene was used as both substrate and extracting agent, avoiding the use of other organic solvents. It permeated through the membrane and solubilised in the aqueous phase, where its photocatalytic conversion to phenol took place. Subsequently the phenol produced during the photocatalytic tests diffused into the organic phase (benzene). Therefore the PMR allowed to obtain phenol production and its separation simultaneously to limit further oxidation to some by-products, like benzoquinone, hydroquinone and other oxidized molecules.

The reduction of pH to 3.1 did not influence significantly the phenol flux $J_{org,Ph}$ with a value of 1.27 mmol $h^{-1}m^{-2}$ with respect to 1.06 mmol $h^{-1}m^{-2}$ at pH 5.5 (Table 6). Nevertheless, the most acidic condition permitted to control the selectivity towards the intermediates, allowing to obtain a lower formation and extraction of these oxidation by-products.

Table 6. Comparison of the results obtained in the photo-oxidation experiments in the PMC at pH 3.1 and 5.5 [4].

	$C_{aq,Ph}$ (mg L^{-1})	$C_{org,Ph}$ (mg L^{-1})	Q_E (%)	$J_{org,Ph}$ (mmol h^{-1} m^{-2})
pH 3.1	16.27	19.04	17.86	1.27
pH 5.5	13.05	17.84	20.25	1.06

The productivity of the system decreased by one order of magnitude by increasing the catalyst concentration from 0.1 to 1.0 g L^{-1} because at the highest catalyst concentration the phenol produced was photodegraded.

As reported by several studies [116, 117], dissolved metal ions influence the photocatalytic reactions because, when they are used in their higher oxidation state, they act as photoelectron acceptors preventing the charge–carrier recombination ($M^{n+} + e \rightarrow M^{(n-1)+}$). Moreover, the reduced species can react with H_2O_2, formed during the reaction [118, 119] to give additional •OH by photo-Fenton reaction ($M^{(n-1)+} + H_2O_2 \rightarrow M^{n+} + \bullet OH + OH^-$). Using salts dissolved in the aqueous phase and iron(III) as dissolved metal ion a positive effect was observed with a phenol flux in the organic phase almost two times greater than those measured without salts as a consequence of the enhanced ionic strength [120, 121].

Summarizing, the possibility to combine heterogeneous photocatalysis with membrane processes using a PMR represents a very promising technology of great research and industrial interest, although much studies are still needed before taking advantage of their potentiality at industrial level.

3.2 PMR in partial oxidation: Conversion of Ferulic acid to vanillin

Vanillin (VA) is one of the most important aromas with an annual world production of about 12,000 t [122-124] and it is widely utilized as a flavoring or functional ingredient in food, cosmetic, pharmaceutical and nutraceutical products [125]. Currently this aromatic aldehyde is mostly synthesized by chemical routes from lignosulfonates of the paper and pulp industry or from guaiacol of petrochemical derivation, but, in these last years the final consumers of VA are becoming more interested in natural products [126, 127] motivating the searcher to find a eco-friendly alternative synthesis of VA. Recently some authors [98, 128, 129] proposed a photocatalytic synthesis of VA, demonstrating that it can be obtained by the photocatalytic

reaction of some precursors, also of natural origin. However, VA is easily degraded into other chemicals. To limit this problem some researchers [98, 129-134] studied a system to enhance the yield of aromatic aldehyde, by coupling the reaction with a membrane separation in a pervaporation photocatalytic reactor (PVPR), so that the produced aldehyde can be recovered during the synthesis to prevent its degradation. Böddeker and coworkers [132-134] demonstrated that membranes in polyether-block-amide (PEBA) are very suitable for pervaporating low volatility aromatics [132] and, in particular, VA [135]. Brazinha et al. [135] analyzed the PV of VA and ferulic acid with polyoctylmethylsiloxane (POMS) membranes, giving an explanation to the high separation factor of VA with respect to ferulic acid.

Camera-Roda et al. [129] demonstrated that the yield of the production of aromatic aldehydes and, specifically, of VA [98] can be enhanced by the coupling of PV with the photocatalytic reaction in the AROMA (Advanced Recovery and Oxidation Method for Aldehydes) process [136, 137]. When photocatalysis is coupled with PV or dialysis, the recovery of the product of the partial oxidation of the aromatic alcohol enhances the rate, the selectivity and the yield. The AROMA process presents an additional list of positive features: straightforward coupling, mild conditions, no chemical additives, "Green" chemicals are produced, semi-continuous (higher productivity) and possibility of operating in a continuous, satisfactory purification of the product, absolute removal of the powders from the product, no effect of the possible fouling, easy control, modularity, it can be applied to the photocatalytic synthesis of a probably large number of aromatic compounds.

Augugliaro et al. [128] reported the photocatalytic oxidation of trans-ferulic acid, isoeugenol, eugenol or vanillyl alcohol to produce VA in aqueous medium by using different TiO_2 samples as photocatalysts. Photocatalytic tests were carried out in two different batch systems: a cylindrical and an annular photoreactor (APR). The authors reported selectivity to VA ranging from 1.4 to 21 mol% during the photo-oxidation tests conducted at room temperature. At the end of the photocatalytic runs of trans-ferulic acid oxidation conducted in the APR, the VA produced was recovered from the aqueous suspension by PV using a non-porous PEBAX® 2533 membrane. This system allowed to obtain also the complete removal of the heterogeneous photocatalyst. They reported that: i) this type of membrane was very selective towards VA, with a transmembrane flux about 3.31 g h^{-1} m^{-2}; ii) in the proposed coupled photocatalysis-PV system the continuous removal of the produced VA from the irradiated suspension avoided its subsequent oxidation, thus increasing the process selectivity. Other important advantage obtained in the proposed system is that the permeated VA vapours were recovered as crystals with a high degree of purity (≥ 99.8%)

by freezing downstream in a liquid nitrogen trap, without the necessity to use complex extraction and re-crystallization procedures.

Camera Roda et al. [129] conducted the photocatalytic tests in a set-up showed in Fig. 14 where the coupling of the two processes was achieved by recirculation in a closed loop of the retentate from the PV modules into the photoreactor and back to PV. The permeate from the PV module, collected by condensation of the permeated vapours, represents the product stream.

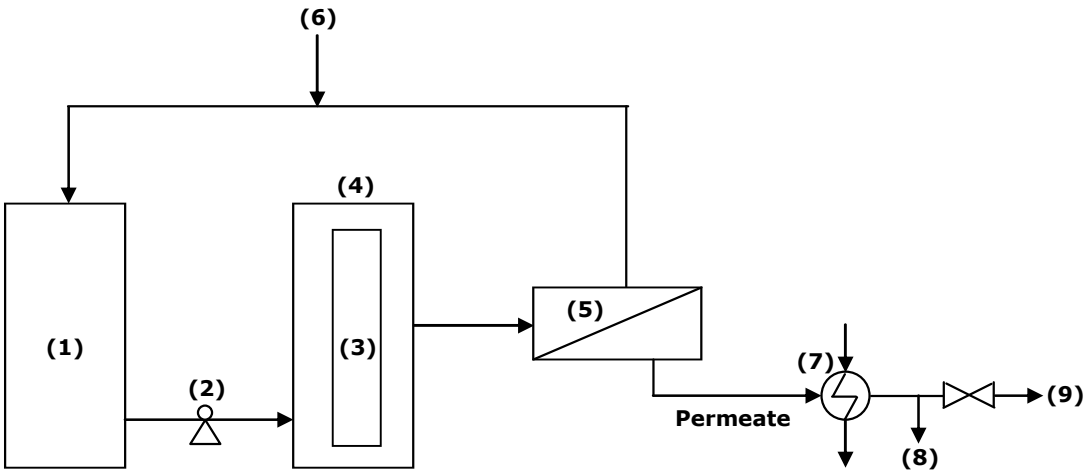

Fig. 14. Scheme of the photocatalytic-pervaporation set-up: (1) thermostated tank; (2) circulation pump; (3) UV lamp; (4) annular photocatalytic reactor; (5) pervaporation unit; (6) optional feed make-up; (7) liquid nitrogen trap; (8) product stream; (9) incondensable (elaborated from [129]).

During preliminary batch photocatalytic tests aldehydes produced are competitive with their corresponding alcohols for the active sites of the semiconductor and then they are degraded by photocatalysis. To extract the product to limit its degradation, some tests were performed in the integrated system (see Fig. 14). In Table 7 the obtained results are compared. Coupling of PV with the photocatalytic partial oxidation of a benzyl alcohol to benzaldehyde the yield of the process and the conversion are enhanced thanks to the continuous recovery of the desired aldehyde, in spite of the little decrease of the selectivity.

Table 7. Conversion, selectivity and yield with and without pervaporation during the photocatalytic conversion of benzyl alcohol to benzaldehyde (Operating condition: volume of the recirculating slurry = 600 mL, catalyst concentration = 0.27 g L^{-1}, temperature = 60 °C, irradiation time = 8 hours, data from [129]).

Operating mode	Conversion (%)	Selectivity (%)	Yield (%)
PC with PV	≈ 35	≈ 17	≈ 6
PC without PV	≈ 22	≈ 18	≈ 3.9

A good integration was achieved even performing photocatalysis and PV in two separate apparatus, provided that the reacting solution is continuously recycled at a sufficiently high flow rate. Additional advantages obtained thanks to this coupling are: i) higher purity of the recovered aldehyde; ii) complete removal of the heterogeneous photocatalyst; iii) semicontinuous production; iv) possibility to maintain mild operative conditions.

In a recent work, Camera-Roda et al. [131] improved the membrane performances in the PV reactor to enhance the VA yield. They quantified, by process simulation, the effect of the enrichment factors and of the permeate flux on the yield in a PV reactor, where VA was produced from ferulic acid and subsequently investigated the methods to enhance these PV performances (enrichment factors and permeate flux) on the basis of the results obtained by process simulation. The study of the VA pervaporation with PEBAX membranes showed that a viable method to enhance the enrichment factor of VA is to increase the membrane thickness, since the resistance to VA permeation remains low while the resistance to water permeation increases. An improvement of the enrichment factor can be obtained also by raising the temperature, with the additional positive effect of increasing the VA flux. The pH has a minor influence on the rejection of the substrate, which remains high also at low pH, when the substrate in solution is not dissociated.

Contrariwise, the permeation of VA is affected by pH. In fact, permeation of VA is relatively high if VA is not dissociated (pH < 6.5), but it decreases at pH = 7.9 when VA is partially dissociated and becomes particularly low when VA is completely dissociated at pH = 10.3. However the real reason for the very high rejection of the substrate (ferulic acid) and of most of the by-products is the low volatility of these compounds.

Summarizing the results obtained by all these authors showed that VA production can be highly enhanced in a PV reactor, where PV recovers VA directly from the reacting solution, thus limiting any further degradation.

3.3 Reduction reactions in a PMR: conversion of acetophenone to phenylethanol

The possibility to use a PMR in reduction reactions was studied very recently by Molinari et al. [99] in the photocatalytic hydrogenation of acetophenone to phenylethanol under UV and visible light. Acetophenone has been used as a model substrate for hydrogenation of aromatic ketones in many studies [138]. The reduction product, phenylethanol, is used as a building block for the synthesis of bioactive compounds such as agrochemicals, pharmaceuticals, and natural products. Indeed, it is a high-value aroma compound with a rose-like odor that is widely used in flavor and fragrance compositions [139]. For most applications natural flavors are preferred, but, owing to limited natural resources of phenylethanol, more production of this compound is required [99].

To make a cheaper and green process the authors used water as solvent, formic acid as hydrogen and electron donor, that is converted into carbon dioxide (CO_2) and hydrogen (H_2) making the reaction irreversible [140, 141]. Commercial TiO_2 as semiconductors and UV light were used to carry out the reaction:

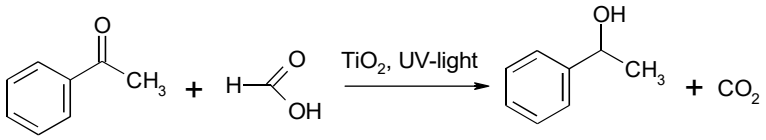

(4)

Solar light contains only 5% of UV radiation. Therefore for any practical application, the photocatalytic system should operate also under visible light. On this basis, to increase the efficiency of TiO_2 under visible light, the authors synthesized titanium dioxide doped with palladium (Pd/TiO_2) by deposition precipitation method.

The preliminary tests, conducted in a batch photoreactor to study the influence of some operating conditions on system performances, showed the best results in terms of phenylethanol yield (4.7%) in the following conditions: i) 1.5 g L^{-1} of TiO_2; ii) pH = 7.5; iii) [HCOOH] = 1.97 M.

Acetophenone reduction was also performed in a PMR, where the photocatalytic process and the separation process allow simultaneously. The tests in the PMR were performed in the experimental set-up schematized in Fig. 15 where the reaction loop is isolated from contact with air. The plant was built by coupling a biphasic membrane contactor (MC) with an APR that consists of a cylindrical pyrex glass reactor with an immersed lamp. The AP, whose volume was 500 mL, was equipped with 3 outputs in its top section for sampling the suspension, for blowing argon and

for degassing air at beginning of the reaction. A peristaltic pump withdraws the aqueous reacting solution from the photocatalytic zone to the separation zone. Then the aqueous phase comes back in the photoreactor by gravity. The MC, immersed in a thermostatic bath was maintained at the same temperature of the photoreactor. It was constituted by two compartment cells (each one with a volume of 130 mL) separated by a flat sheet polypropylene membrane with an exposed membrane surface area of 28.3 cm^2. The first compartment contains the aqueous reacting phase coming from the photoreactor, while the second one contains an organic extracting phase mechanically stirred by a motor. The phenylethanol produced in the aqueous reacting phase diffuses through the membrane and then dissolves into the organic extracting phase, where it is protected by successive over-hydrogenation, which can result in an enhancement of process selectivity. The use of a membrane extractor instead of a traditional liquid/liquid extraction unit avoids physical mixing between the organic and the aqueous phases, and allows a continuous extraction process.

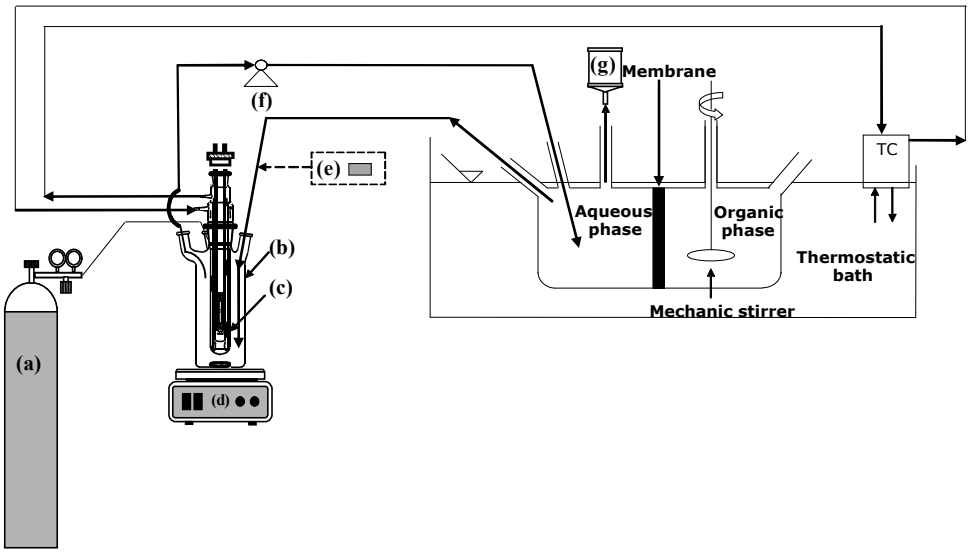

Fig. 15. Scheme of the membrane contactor integrated with the annular photoreactor: (a) argon cylinder; (b) annular photoreactor; (c) medium pressure Hg lamp with cooling jacket; (d) magnetic stirrer; (e) optional syringe pump for substrate feeding; (f) peristaltic pump; (g) degassing system; (TC) temperature controller [99].

The results obtained during the photocatalytic hydrogenation tests on acetophenone in the PMR compared with that one obtained under the same operating conditions in the batch system showed that using the PMR the substrate conversion, yield, produced amount of phenylethanol

and overall phenol productivity improve. This behaviour is caused by the simultaneous extraction of phenylethanol in the organic phase that shifts the reaction forward to the product. Moreover, the extraction of phenylethanol from the reactive phase allows to avoid a subsequent reduction reaction of the extracted product enhancing the selectivity value.

During the experimental tests conducted in the PMR under UV light, the influence of various reaction parameters such as different substrate feeding mode, addition of triethylamine, and different flow rates were investigated in order to improve the phenylethanol productivity and its extraction percentage into the organic extracting phase.

The feeding modes of the substrate were: i) drop by drop by the syringe pump; ii) dissolved in n-heptane; iii) reactant and organic extracting phase. The most efficient system was found to be the membrane reactor in which the acetophenone was used as both substrate and organic phase (276.20 µmol of phenyl ethanol generated, 4.44 $mg_{prod}\ g_{cat}^{-1}h^{-1}$ phenylethanol productivity, 21.91% extraction percentage). This system permitted to obtain both the best substrate solubilisation in the reacting phase and the best product extraction in the organic phase (Fig. 16). Furthermore, by using n-heptane as solvent the final organic phase was mainly constituted by three components (acetophenone, phenylethanol and heptane) whilst by operating in the reactant and extractant mode the final organic phase was mainly constituted by two components (acetophenone and phenylethanol). This makes easier the subsequent product recovery. Moreover acetophenone is less volatile than heptane (boiling point 202 °C versus 98-99 °C), thus allowing to perform the reaction for long irradiation time by working continuously.

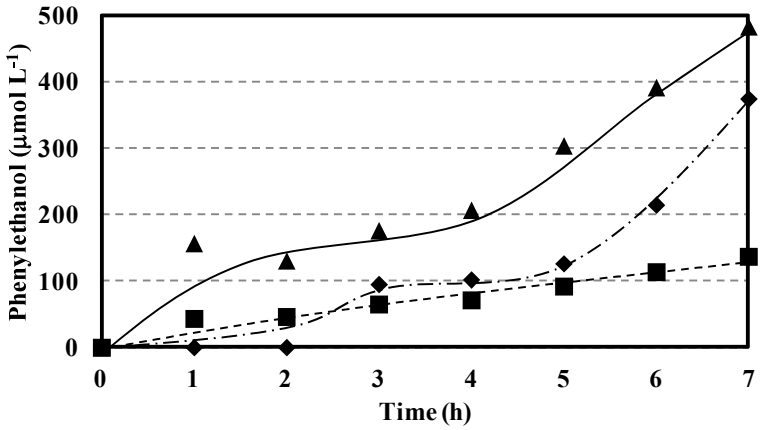

Fig. 16. Phenylethanol concentration in the organic phase vs. time by using the membrane photoreactor with different substrate feeding mode: syringe pump (♦), acetophenone dissolved in n-heptane (■), acetophenone as reactant and extractant (▲) [99].

Tests conducted under visible light showed that TiO_2 was not active under visible light irradiation, while doping the commercial catalyst with Pd the concentration of phenylethanol in the organic phase increased linearly during the photocatalytic test (Fig. 17).

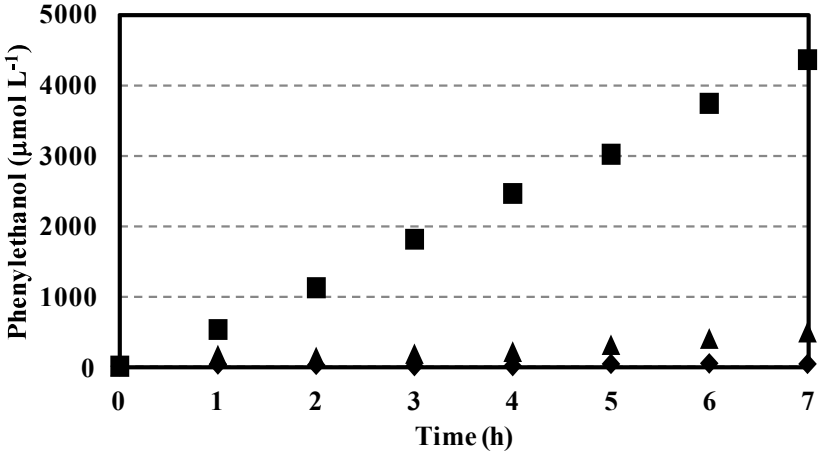

Fig. 17. Phenylethanol extraction in the organic phase vs. time by using TiO_2 (♦) and Pd/TiO_2 (■) under visible light and TiO_2 under UV light (▲) [99].

The superior activity of this Pd/TiO_2 was determined considering the phenyethanol production by using Pd/TiO_2 that was higher than the amount of desired product obtained in all tests conducted under UV light. The Pd/TiO_2 was active under visible light producing a greater amount of phenylethanol (1371 µmol) and giving a productivity (22.02 $mg_{prod}\ g_{cat}^{-1}h^{-1}$) five times higher than that obtained by using the bare TiO_2 under UV light for the photocatalytic hydrogenation of acetophenone conducted in the same PMR system.

Summarizing, the results evidenced that use of a PMR, coupling the photocatalytic reduction with a membrane separation system, allows to improve substrate conversion, yield, produced amount of phenylethanol and the overall phenol productivity. Indeed the use of Pd/TiO_2 photocatalyst permitted to efficiently carry out the photocatalytic hydrogenation of acetophenone to phenylethanol under visible light. This approach will allow to make a green and sustainable process.

4. Conclusion

Photocatalytic Membrane Reactors (PMRs) have been experimented with interesting results in the photodegradation of organic pollutants as well as in the synthesis of organic compounds by partial oxidation or partial hydrogenation.

PMRs, thanks to the selective properties of the membrane, permit to achieve continuous operation in a system that allows not only the recovery and reuse of the photocatalyst (in suspension or immobilized) but also enhance the residence time of the substrate(s) to be converted (total or partial oxidation or reduction) and allows a selective separation of the product(s).

The various described configurations of PMRs can influence the performance of the photocatalytic systems and control the catalyst activity, the fouling, the selectivity and the rejection of the membrane.

In the PMR configurations using suspended photocatalyst, the photocatalytic zone can be separated by the separation zone, giving some important advantages like the possibility to use commercial membranes/modules. Membrane fouling and light scattering represent the most important aspect to be taken into account, affecting the photocatalytic performance of the system. In the case of photocatalytic degradation processes, the use of a submerged photocatalytic membrane reactor (SPMR) with air bubbling and adequate membrane back-flushing represents the configuration showing, at the present, greater perspectives at large scale level.

In the case of PMRs with immobilized photocatalyst, the preparation of photocatalytic membrane systems, with suitable pore size and effective dispersion of the catalyst particles, represents an important challenge to contrast the loss of photoactivity related to both the low photocatalyst availability to irradiation and mass transfer limitations. In this system the irradiation of the photocatalytic membrane is required, which can result in membrane and/or photocatalyst degradation. The use of TiO_2 nanoparticles immobilized in/on inorganic membranes represents an interesting approach responding to these requirements.

SPMRs can have, at present, greater perspective of industrial applications. Indeed, use of commercial membranes and possibility to separate the reaction zone from the separation zone are two important design aspects.

The results obtained on the synthesis of organic compounds such as phenol, vanillin and phenylethanol in PMRs show further applications and perspectives of this type of hybrid process.

The possibility to use the Sun as a cheap and clean source of light has to be considered in view of developing photocatalysts working with visible light thus making a more sustainable process. PMRs can be considered a useful "green" integrated system for water purification as well as for organic synthesis, although additional studies are still needed to take advantage of their potentiality at industrial level.

5. List of symbols

AOP:	Advanced Oxidation Process
APR:	Annular Photocatalytic Reactor
AR1:	Acid Red 1
AR18:	Acid Red 18
AROMA:	Advanced Recovery and Oxidation Method for Aldehydes
AY36:	Acid Yellow 36
BET:	Brunauer–Emmett–Teller
BSA:	Bovine Serum Albumin
CB:	Conduction Band
CMD:	Cimetidine
4-CP:	4-chlorophenol
CR:	Congo Red
CVD:	Chemical Vapor Deposition
DCF:	Diclofenac
DCMD:	Direct Contact Membrane Distillation
DG99:	Direct Green 99
2,4-DHBA:	2,4-dihydroxybenzoic acid
DPH:	Diphenhydramine
DW:	Distilled Water
Eg:	Band gap energy level
GEM:	Gemfibrozil
GO:	Graphene Oxide
GO-TiO_2:	Graphene Oxide doped TiO_2
GW:	Groundwater
HA:	Humic Acids

1329	HFM:	Hollow Fiber Membrane
1330	IBU:	Ibuprofen
1331	K_D:	Partition coefficient
1332	LIN:	Lincomycin
1333	MB:	Methylene Blue
1334	MC:	Membrane Contactor
1335	MD:	Membrane Distillation
1336	MO:	Methyl Orange
1337	NaA:	Sodium Alginate
1338	NAP:	Naproxen
1339	NF:	Nanofiltration
1340	NOM:	Natural Organic Matter
1341	N-TiO_2:	Nitrogen doped TiO_2
1342	PhACs:	Pharmaceutically Active Compounds
1343	PB:	Patent Blue
1344	PC:	Photocatalysis
1345	Pd/TiO_2:	Palladium doped TiO_2
1346	PE:	Primary Effluent
1347	PEBA:	Polyether-Block-Amide
1348	PES:	Polyethersulfone
1349	POMS:	Polyoctylmethylsiloxane
1350	PM:	Photocatalytic Membrane
1351	PMC:	Photocatalytic Membrane Contactor
1352	PMR:	Photocatalytic Membrane Reactor
1353	PR:	Photoreactor
1354	PV:	Pervaporation
1355	PVDF:	Polyvinylidene fluoride
1356	PVDF-NFs:	Polyvinylidene fluoride nanofibers
1357	PVPR:	Pervaporation Photocatalytic Reactor
1358	SBW:	Simulated Brackish Water
1359	SC:	Semiconductor
1360	SE:	Secondary Effluent

SEM: Scanning Electron Microscopy

SPMR: Submerged Photocatalytic Membrane Reactor

SSF: Stainless Steel Filter

SW: Seawater

TAM: Tamoxifene

TCEP: Tris(2-chloroethyl) phosphate

TiO_2-NFs: TiO_2 nanofibers

TMP: Transmembrane Pressure

TOC: Total Organic Carbon

TrOCs: Trace Organic Contaminants

TTIP: Titanium Tetraisopropoxide

TW: Tap Water

UV: Ultraviolet radiation

UW: Ultrapure Water

UF: Ultrafiltration

VA: Vanillin

Vis: Visible radiation

VB: Valence Band

XRD: X-ray Powder Diffraction

6. References

[1] A. Fujishima, K. Honda, Nature 238 (1972) 37-38.

[2] G. Palmisano, E. Garcıa-Lopez, G. Marcì, V. Loddo, S. Yurdakal, V. Augugliaro, L. Palmisano, Chem. Commun. 46 (2010) 7074-7089.

[3] J.J. Murcia, M.C. Hidalgo, J.A. Navío, J. Araña, J.M. Doña-Rodríguez, Appl. Catal. B-Environ. 179 (2015) 305-312.

[4] R. Molinari, A. Caruso, T. Poerio, Catal. Today 144 (2009) 81–86.

[5] R. Molinari, P. Argurio, C. Lavorato, Curr. Org. Chem. 17 (2013) 2516-2537.

[6] J.-M. Herrmann, Top. Catal. 34 (2005) 49-65.

[7] D. Lu, P. Fang, X. Liu, S. Zhai, C. Li, X. Zhao, J. Ding, R. Xiong, Appl. Catal. B-Environ. 179 (2015) 558–573.

[8] X. Hou, H. Ma, F. Liu, J. Deng, Y. Ai, X. Zhao, D. Mao, D. Li, B. Liao, J. Hazard. Mater. 299 (2015) 59–66.

[9] M.D. Hernández-Alonso, F. Fresno, S. Suárez, J.M. Coronado, Energ. Environ. Sci. 2 (2009) 1231–1257.

[10] R. Molinari, P. Argurio, L. Palmisano, Photocatalytic membrane reactors for water treatment, in: A. Basile, A. Cassano, N.K. Rastogi (Eds.), Advances in Membrane Technologies for Water Treatment - Materials, Processes and Applications, Woodhead Publishing Series in Energy: Number 75, Elsevier Ltd. - Woodhead Publishing Limited, Cambridge, 2015, pp. 205-238.

[11] S. Gazi, R. Ananthakrishnan, Appl. Catal. B-Environ. 105 (2011) 317–325.

[12] S.O. Flores, O. Rios-Bernij, M.A. Valenzuela, I. Cordova, R. Gomez, R. Gutierrez, Top. Catal. 44 (2007) 507-511.

[13] G. Palmisano, V. Augugliaro, M. Pagliaro, L. Palmisano, Chem. Commun. (2007) 3425–3437.

[14] R. Molinari, A. Caruso, L. Palmisano, Photocatalytic Processes in Membrane Reactors, in: E. Drioli, L. Giorno (Eds.), Comprehensive Membrane Science and Engineering, Vol. 3, Elsevier Science B.V., Oxford, 2010, pp. 165-193.

[15] M. Ni, M.K.H. Leung, D.Y.C. Leung, K. Sumathy, Renew. Sust. Energ. Rev. 11 (2007) 401-425.

[16] R. Molinari, A. Caruso, P. Argurio, T. Poerio, J. Membrane Sci. 319 (2008) 54-63.

[17] G. Mascolo, R. Comparelli, M.L. Curri, G. Lovecchio, A. Lopez, A. Agostiano, J. Hazard. Mater. 142 (2007) 130-137.

[18] R. Molinari, F. Pirillo, M. Falco, V. Loddo, L. Palmisano, Chem. Eng. Process. 43 (2004) 1103-1114.

[19] R. Molinari, L. Palmisano, E. Drioli, M. Schiavello, J. Membrane Sci. 206 (2002) 399-415.

[20] M.F.J. Dijkstra, H. Buwalda, A.F. de Jong, A. Michorius, J.G.M. Wilkelman, A.A.C.M. Beenackers, Chem. Eng. Sci. 56 (2001) 547-555.

[21] Y. Huo, Z. Xie, X. Wang, H. Li, M. Hoang, R.A. Caruso, Dyes Pigments 98 (2013) 106-112.

[22] S. Mozia, A.W. Morawski, Catal. Today 118 (2006) 181-188.

[23] S. Mozia, D. Darowna, J. Przepiórski, A.W. Morawski, Pol. J. Chem. Technol. 15 (2013) 51-60.

[24] W. Baran, A. Makowski, W. Wardas, Dyes Pigm. 76 (2008) 226-230.

[25] X. Yang, L. Xu, X. Yu, Y. Guo, Catal. Commun. 9 (2008) 1224-1229.

[26] Z. Sha, H.S.O. Chan, J. Wu, J. Hazard. Mater. 299 (2015) 132-140.

[27] A. Samadi-Maybodi, M.R. Sadeghi-Maleki, Spectrochim. Acta A 152 (2016) 156-164.

[28] L. Lhomme, S. Brosillon, D. J. Wolbert, J. Photochem. Photobiol. A-Chem., 188 (2007) 34-42.

[29] R. Molinari, F. Pirillo, V. Loddo, L. Palmisano, Catal. Today 118 (2006) 205-213.
[30] S. Yurdakal, V. Loddo, V. Augugliaro, H. Berber, G. Palmisano, L. Palmisano, Catal. Today 129 **(**2007) 9-15.
[31] J.C. Ahern, R. Fairchild, J.S. Thomas, J. Carr, H.H. Patterson, Appl. Catal. B-Environ. 179 (2015) 229-238.
[32] M. Długosz, P. Zmudzki, A. Kwiecien, K. Szczubiałka, J. Krzek, M. Nowakowska, J. Hazard. Mat. 298 (2015) 146–153.
[33] Y. Zhang, J.L. Zhou, B. Ning, Water Res. 41 (2007) 19-26.
[34] X. Huang, M. Leal, Q. Li, Water Res. 42 (2008) 1142-1150.
[35] A. Lair, C. Ferronato, J.-M. Chovelon, J.-M. Herrmann, J. Photochem. Photobiol. A-Chem. 193 (2008) 193-203.
[36] J. Ye, X. Li, J. Hong, J. Chen, Q. Fan, Mat. Sci. Semicon. Proc. 39 (2015) 17-22.
[37] D. Zhang, J. Wang, J. Water Process Eng. 7 (2015) 187-195.
[38] N. Demir, G. Gündüz, M. Dükkancı, Environ. Sci. Pollut R. 22 (2015) 3193-3201.
[39] D. Das, R.K. Dutta, J. Colloid Interf. Sci. 457 (2015) 339-344.
[40] A.K. Verma, R.R. Dash, P. Bhunia, J. Environ. Manage. 93 (2012) 154–168.
[41] C.-Z. Liang, S.-P. Sun, F.-Y. Li, Y.-K. Ong, T.-S. Chung, J. Membrane Sci. 469 (2014) 306–315.
[42] J. Dasgupta, J. Sikder, S. Chakraborty, S. Curcio, E. Drioli, J. Environ. Manage. 147 (2015) 55–72.
[43] J. Tian, Y. Leng, H. Cui, H. Liu, J. Hazard. Mater. 299 (2015) 165-173.
[44] P. Bansal, G.R. Chaudhary, S.K. Mehta, Chem. Eng. J. 280 (2015) 475-485.
[45] R. Molinari, F. Pirillo, M. Falco, V. Loddo, L. Palmisano, Chem. Eng. & Processing 43 (2004) 1103-1114.
[46] N.H.H. Hairom, A.W. Mohammad, L.Y. Ng, A.A.H. Kadhumb, Desal. Wat. Treatment 54 (2015) 944–955.
[47] K. Sopajaree, S.A. Qasim, S. Basak, K. Rajeshwar, J. Appl. Electrochem. 29 (1999) 1111-1118.
[48] S. Kertèsz, J. Cakl, H. Jiránková, Desalination 343 (2014) 106–112.
[49] H. Zhang, X. Quan, S. Chen, H. Zhao, Y. Zhao, Sep. Purif. Technol. 50 (2006) 147–155.
[50] C.P.Athanasekou, N.G.Moustakas, S. Morales-Torres, L.M. Pastrana-Martínez, J.L. Figueiredo, J.L. Faria, A.M.T. Silva, J.M. Dona-Rodriguez, G.E. Romanos, P. Falaras, Appl. Catal.B-Environ. 178 (2015) 12–19.

[51] Z.-B. Wang, Y.-J. Guan, B. Chen, S.-L. Bai, Desal. Water Treat., Published online: 28 Aug 2015, DOI: 10.1080/19443994.2015.1082940.
[52] L.M. Pastrana-Martìnez, S. Morales-Torres, J.L. Figueiredo, J.L. Faria, A.M.T. Silva, Water Res. 77 (2015) 179-190.
[53] S.K. Papageorgiou, F.K. Katsaros, E.P. Favvas, G.E. Romanos, C.P. Athanasekou, K.G. Beltsios, O.I. Tzialla, P. Falaras, Water Res. 46 (2012) 1858-1872.
[54] L. Liu, Z. Liu, H. Bai, D.D. Sun, Water Res. 46 (2012) 1101-1112.
[55] S. Mozia, M. Tomaszewska, A.W. Morawski, Appl. Catal. B-Environ. 59 (2005) 131–137.
[56] S. Mozia, M. Tomaszewska, A.W. Morawski, Catal. Today 129 (2007) 3–8.
[57] J. Fu, M. Ji, Z. Wang, L. Jin, D. An, J. Hazard. Mater. 131 (2006) 238–242.
[58] S.S. Chin, T.M. Lim, K. Chiang, A.G. Fane, Desalination 202 (2007) 253–261.
[59] X. Huang, Y. Meng, P. Liang, Y. Qian, Sep. Purif. Technol. 55 (2007) 165–172.
[60] S.O. Ganiyu, E.D. van Hullebusch, M. Cretin, G. Esposito, M.A. Oturan, Sep. Purif. Technol. 156 (2015) 891–914.
[61] M.A. Anderson, M.J. Gieselmann, Q.J. Xu, J. Membrane Sci. 39 (1988) 243–258.
[62] M.D. Moosemiller, C.G. Hill (Jr.), M.A. Anderson, Sep. Sci. Technol. 24 (1989) 641–657.
[63] S. Ramasundaram, H.N. Yoo, K.G. Song, J. Lee, K.J. Choi, S.W. Hong, J. Hazard. Mater. 258–259 (2013) 124–132.
[64] A. Georgi, F.-D. Kopinke, Appl. Catal. B-Environ. 58 (2005) 9–18.
[65] A.Y. Shan, T.I.M. Ghazi, S.A. Rashid, Appl. Catal. A-Gen. 389 (2010) 1–8.
[66] N. Ma, Y. Zhang, X. Quan, X. Fan, H. Zhao, Water Res. 44 (2010) 6104–6114.
[67] J. Yu, J. Xiong, B. Cheng, S. Liu, Appl. Catal. B-Environ. 60 (2005) 211–221.
[68] Q.A.H. Jones, N. Voulvoulis, J.N. Lester, Water Res. 36 (2002) 5013-5022.
[69] B. Kasprzyk-Hordern, R.M. Dinsdale, A.J. Guwy, Water Res. 42 (2008) 3498-3518.
[70] F. Pietrini, D. Di Baccio, J. Acena, S. Pérez, D. Barceló, M. Zacchini, J. Hazard. Mat. 300 (2015) 189-193.
[71] A. Nikolaou, S. Meric, D. Fatta, Anal. Bioanal. Chem. 387 (2007) 1225-1234.
[72] E.V. dos Santos, C. Sáez, C.A. Martínez-Huitle, P. Cañizares, M.A. Rodrigo, J. Hazard. Mat. 300 (2015) 129-134.
[73] T. Heberer, Toxicol. Lett. 131 (2002) 5-17.
[74] E. Zuccato, S. Castiglioni, R. Fanelli, J. Hazard. Mater. 122 (2005) 205-209.

[75] M.J. Gomez, M.J. Martınez Bueno, S. Lacorte, A.R. Fernandez-Alba, A. Aguera, Chemosphere 66 (2007) 993-1002.
[76] R. Molinari, P. Argurio, T. Poerio, J. Membrane Sci. 340 (2009) 26-34.
[77] M.C. Ncibi, M. Sillanpää, J. Hazard. Mat. 298 (2015) 102–110.
[78] V. Augugliaro, E. Garcia-Lopez, V. Loddo, S. Malato Rodriguez, I. Maldonado, G. Marcì, R. Molinari, L. Palmisano, Sol. Energy 79 (2005) 402-408.
[79] R. López Fernandez , J.A. McDonald, S.J. Khan, P. Le-Clech, Sep. Purif. Technol. 127 (2014) 131–139.
[80] V.C. Sarasidis, K.V. Plakas, S.I. Patsios, A.J. Karabelas, Chem. Eng. J. 239 (2014) 299-311.
[81] K. Fischer, M. Grimm, J. Meyers, C. Dietrich, R. Gläser, A. Schulze, J. Membrane Sci. 478 (2015) 49–57.
[82] K. Fischer, M. Kuhnert, R. Glaser, A. Schulze, RSC Adv. 5 (2015) 16340-16348.
[83] S. Mozia, A.W. Morawski, Catal. Today 193 (2012) 213-220.
[84] D. Darowna, S. Grondzewska, A.W. Morawski, S. Mozia, J. Chem. Technol. Biotechnol. 89 (2014) 1265-1273.
[85] M.N. Chong, B. Jin, C.W.K. Chow, C. Saint, Water Res. 44 (2010) 2997–3027.
[86] A. Sotto, A. Boromand, S. Balta, J. Kim, B. Van der Bruggen, J. Mater. Chem. 21 (2011) 10311-10320.
[87] A. Razmjou, J. Mansouri, V. Chen, M. Lim, R. Amal, J. Membrane Sci. 380 (2011) 98–113.
[88] P. Petrochenko, G. Scarel, G.K. Hyde, G. Parsons, S. Skoog, Q. Zhang, P. Goering, R. Narayan, JOM 65 (2013) 550–556.
[89] W. Krengvirat, S. Sreekantan, A.-F. Mohd Noor, N. Negishi, G. Kawamura, H. Muto, A. Matsuda, Mater. Chem. Phys. 137 (2013) 991–998.
[90] K. Nakata, A. Fujishima, J. Photochem. Photobiol. C 13 (2012) 169–189.
[91] H. Degaard, B. Eikebrokk, R. Storhaug, Wat. Sci. Technol. 40 (1999) 37–46.
[92] A. Ding Nian, Technol. Water Treatment 1 (1982) 7–11.
[93] X. Zheng, Q. Wang, L. Chen, J. Wang, R. Cheng, Chem. Eng. J. 277 (2015) 124–129.
[94] K. Azrague, P. Aimar, F. Benoit-Marquié, M.T. Maurette, Appl. Catal. B-Environ. 72 (2007) 197-204.
[95] G. Camera-Roda, F. Santarelli, J. Sol. En. Eng. 129 (2007) 68-73.
[96] J. Li, J. Yang, F. Wen, C. Li, Chem. Commun. 47 (2011) 7080-7082.

[97] J.M. Herrmann, C. Duchamp, M. Karkmaz, B. Thu Hoai, H. Lachheb, E. Puzenat, C. Guillard, Materials 146 (2007) 624-629.
[98] G. Camera-Roda, V. Augugliaro, A. Cardillo, V. Loddo, G. Palmisano, L. Palmisano, Chem. Eng. J. 224 (2013) 136-143.
[99] R. Molinari, C. Lavorato, P. Argurio, Chem. Eng. J. 274 (2015) 307-316.
[100] J. Coronas, J. Santamaria, Catal. Today 51 (1999) 377-389.
[101] J.N. Armor, J. Membrane Sci. 147 (1998) 217-233.
[102] R. Molinari, C. Lavorato, T. Poerio, Appl. Catal. A-Gen. 417 (2012) 87-92.
[103] Y. Liu, K. Murata, M. Inaba, J. Mol. Catal. A-Chem. 256 (2006) 247–255.
[104] R. Molinari, P. Argurio, T. Poerio, J. Membrane Sci. 476 (2015) 490-499.
[105] S. Niwa, M. Eswaramoorthy, J. Nair, A. Raj, N. Itoh, H. Shoji, T. Namba, F. Mizuka, Science 295 (2002) 105–107.
[106] G. Bellussi, C. Perego, CATTECH 4 (2000) 4–16.
[107] G.I. Panov, CATTECH 4 (2000) 18–32.
[108] D. Bianchi, L. Balducci, R. Bortolo, R. D'Aloisio, M. Ricci, G. Span, R. Tassinari, C. Tonini, R. Ungarelli, Adv. Synth. Catal. 349 (2007) 979–986.
[109] R. Molinari, T. Poerio, Asia-Pac. J. Chem. Eng. 5 (2010) 191–206.
[110] N. Itoh, S. Niwa, F. Mizukami, T. Lnoue, A. Igarashi, T. Namba, Catal. Commun. 4 (2003) 243–246.
[111] W. Laufer, W.F. Helderich, Chem. Commun. (2002) 1684–1685.
[112] D. Bianchi, R. Bortolo, R. Tassinari, M. Ricci, R. Vignola, Angew. Chem. Int. Edit. 39 (2000) 4321–4323.
[113] R. Cai, S. Song, B. Ji, W. Yang, G. Sun, Q. Xin, Catal. Today 104 (2005) 200–204.
[114] X.B. Wang, Y. Guo, X.F. Zhang, H. Liu, J. Wang, K.L. Yeung, Catal. Today 156 (2010) 288–294.
[115] X.B. Wang, X.F. Zhang, H. Liu, K.L. Yeung, J.Q. Wang, Chem. Eng. J. 156 (2010) 562–570.
[116] V. Brezova, A. Blazkova, E. Borosova, M. Ceppan, R. Fiala, J. Mol. Catal. A-Chem. 98 (1995) 109-116.
[117] J. Sykora, M. Pado, M. Tatarko, M. Izakovic, J. Photoch. Photobio. A 110 (1997) 167-175.
[118] K. Kavita, C. Rubina, L.S. Rameshwar, Ind. Eng. Chem. Res. 43 (2004) 7683-7696.
[119] I.K. Konstantinou, T.A. Albanis, Appl. Catal. B-Environ. 49 (2004) 1-14.
[120] A. Noubigh, A. Mgaidi, M. Abderrabba, E. Provost, W.J. Fürst, J. Sci. Food. Agr. 87 (2007) 783-788.

[121] A. Noubigh, M. Abderrabba, E. Provost, J. Chem. Thermodyn. 39 (2007) 297-303.
[122] N.J. Walton, M.J. Mayer, A. Narbad, Vanillin, Phytochemistry 63 (2003) 505–515.
[123] H. Korthou, R. Verpoorte, Vanilla, in: R.G. Berger (Ed.), Flavours and Fragrances, Springer-Verlag Berlin Heidelberg, 2007, pp. 203–217.
[124] S.R. Rao, G.A. Ravishankar, J. Sci. Food Agric. 80 (2000) 289–304.
[125] A.K. Sinha, U.K. Sharma, N. Sharma, Int. J. Food Sci. Nutr. 59 (2008) 299–326.
[126] M. Laroche, J. Bergeron, G. Barbaro-Forleo, J. Consum. Market. 18 (2001) 503–520.
[127] J. Pickett-Baker, R. Ozaki, J. Consum. Market. 25 (2008) 281–293.
[128] V. Augugliaro, G. Camera-Roda, V. Loddo, G. Palmisano, L. Palmisano, F. Parrino, M.A. Puma, Appl. Catal. B-Environ. 111 (2012) 555–561.
[129] G. Camera-Roda, F. Santarelli, V. Augugliaro, V. Loddo, G. Palmisano, L. Palmisano, S. Yurdakal, Catal. Today 161 (2011) 209–213.
[130] G. Camera Roda, F. Santarelli, Chem. Eng. Technol. 35 (2012) 1221–1228.
[131] G. Camera-Roda, A. Cardillo , V. Loddo , L. Palmisano, F. Parrino., Membranes 4 (2014) 96-112.
[132] K.W. Böddeker, G. Bengston, E. Bode, J. Membrane Sci. 53 (1990) 143–158.
[133] K.W. Böddeker, G. Bengston, H. Pingel, S. Dozel, Desalination 90 (1993) 249–257.
[134] K.W. Böddeker, I.L. Gatfield, J. Jähnig, C. Schorm, J. Membrane Sci. 137 (1997) 155–158.
[135] C. Brazhina, B. Barbosa, G.J. Crespo, Green Chem. 13 (2011) 2197–2203.
[136] G. Camera-Roda, V. Augugliaro, V. Loddo, G. Palmisano, L. Palmisano, U.S. Patent 20130123546 A1, 10 June 2011.
[137] G. Camera-Roda, V. Augugliaro, V. Loddo, L. Palmisano, Pervaporation membrane reactors, in: A. Basile (Ed.), Handbook of Membrane Reactors. Volume 2: Reactor types and industrial applications, Woodhead Publishing Limited, Cambridge, 2013, pp. 107 – 151.
[138] S. Kohtani, E. Yoshioka, K. Saito, A. Kudo, H. Miya, Catal. Commun. 11 (2010) 1049–1053.
[139] R. Molinari, C. Lavorato, T.F. Mastropietro, P. Argurio, E. Drioli, T. Poerio, Molecules 21 (2016) 394, doi:10.3390/molecules21030394.
[140] K. Imamura, S. Iwasaki, T. Maeda, K. Hashimoto, B. Ohtani, H. Kominami, Phys. Chem. Chem. Phys. 13 (2011) 5114– 5119.
[141] N. Wehbe, M. Jaafar, C. Guillard, J.-M. Herrmann, S. Miachon, E. Puzenat, N. Guilhaume, Appl. Catal. A-Gen. 368 (2009) 1–8.